Neutrino Oscillations and Collider Test of the R-parity Violating Minimal Supergravity Model

Dong-Won Jung[1], Sin Kyu Kang[2], Jong Dae Park[3] and Eung Jin Chun[4]
[1] *Department of Physics, Korea Advanced Institute of Science and Technology, 373-1 Kusong-dong, Yusong-gu, Daejoen 305-701, Korea*
[2]*School of Physics, Seoul Nat'l University, Seoul 151-747, Korea*
[3]*Institute of Physics and Applied Physics, Yonsei University, Seoul 120-749, Korea*
[4]*Korea Institute for Advanced Study, 207-43 Cheongryangri-dong, Dongdaemun-gu, Seoul 130-722, Korea*

We study the R-parity violating minimal supergravity models accounting for the observed neutrino masses and mixing, which can be tested in future collider experiments. The bi-large mixing can be explained by allowing five dominant tri-linear couplings $\lambda'_{1,2,3}$ and $\lambda_{1,2}$. The desired ratio of the atmospheric and solar neutrino mass-squared differences can be obtained in a very limited parameter space where the tree-level contribution is tuned to be suppressed. In this allowed region, we quantify the correlation between the three neutrino mixing angles and the tri-linear R-parity violating couplings. Qualitatively, the relations $|\lambda'_1| < |\lambda'_2| \sim |\lambda'_3|$, and $|\lambda_1| \sim |\lambda_2|$ are required by the large atmospheric neutrino mixing angle θ_{23} and the small angle θ_{13}, and the large solar neutrino mixing angle θ_{12}, respectively. Such a prediction on the couplings can be tested in the next linear colliders by observing the branching ratios of the lightest supersymmetric particle (LSP). For the stau or the neutralino LSP, the ratio $|\lambda_1|^2 : |\lambda_2|^2 : |\lambda_1|^2 + |\lambda_2|^2$ can be measured by establishing $Br(e\nu) : Br(\mu\nu) : Br(\tau\nu)$ or $Br(\nu e^\pm \tau^\mp) : Br(\nu\mu^\pm\tau^\mp) : Br(\nu\tau^\pm\tau^\mp)$, respectively. The information on the couplings λ'_i can be drawn by measuring $Br(l_i t\bar{b}) \propto |\lambda'_i|^2$ if the neutralino LSP is heavier than the top quark.

PACS numbers: 12.60.-i, 14.60.St

I. INTRODUCTION

The recent progress in neutrino experiments has established the picture for three active neutrino oscillations [1], which requires new physics beyond the Standard Model. The supsersymmetric standard model (SSM) would be the best motivated candidate for new physics. In the SSM, the lepton and baryon number conservation is not guaranteed by the gauge symmetry and thus one usually imposes an extra global symmetry, the R-parity, to forbid the fast proton decay. However, the proton longevity can be ensured by imposing only the baryon number symmetry. Then, the neutrino masses and mixing could be the consequence of the lepton number violation in the SSM. In this respect, the R-parity violating SSM has been extensively examined [2].

The phenomenological study of the SSM strongly depends on the mechanism of supersymmetry (SUSY) breaking. The most popular scenario would have been the minimal supergravity model (mSUGRA) in which the universality of the soft supersymmetry breaking terms is introduced to solve the supersymmetric flavor problem. The mSUGRA model is highly predictive as it contains only 3 independent soft parameters: a universal gaugino mass $M_{1/2}$, a universal scalar mass m_0, a universal trilinear coupling A_0 at the ultraviolet scale. The R-parity conserving mSUGRA model has been one of the most popular model as it contains a natural dark matter candidate of the Universe, the lightest supersymmetry particle (LSP), on top of its simplicity and predictability. Allowing R-parity violation in the mSUGRA model, such a feature is lost but the LSP can produce clean lepton number violating signals through its decay [3], which provides a definite collider test of the model as the origin of the neutrino masses and mixing [4, 5, 6, 7, 8, 9].

This article aims at an extensive investigation of the mSUGRA model with R-parity violation. We will first analyze the parameter space of the model in which the phenomenological neutrino mass matrix consistent with the present neutrino experimental results can be accommodated. Concerning this, one may separate two issues: realizing (i) two large and one small mixing angles, and (ii) a mild hierarchy between the atmospheric and the solar neutrino mass scales. The property (i) can be explained simply by introducing an appropriate lepton flavor structure of the tri-linear R-parity violating couplings [7, 10]. Here, let us remark that the bi-large mixing can also be realized with allowing only the bilinear R-parity violating terms if one introduces non-universality in the soft terms [11, 12, 13]. It is however non-trivial to achieve (ii) as the mSUGRA model generically predicts very small values of $\Delta m^2_{sol}/\Delta m^2_{atm}$ where the atmospheric mass splitting Δm^2_{atm} comes basically from the tree-level contribution over-dominating the loop corrections which are supposedly responsible for the solar neutrino mass splitting Δm^2_{sol}. As a consequence, we find a very limited region of the parameter space consistent with neutrino experimental results. This is an undesirable feature of the mSUGRA scenario for the neutrino masses and mixing compared with other scenarios such as gauge-mediated SUSY breaking model [7].

Given the allowed region of the (R-parity conserving and violating) parameter space, we will then examine various

ways to test the model in the future colliders through the decays of the LSP, which can be either a neutralino or a stau. As discussed in Refs. [4, 5, 6, 7, 8, 9], in models of neutrino masses and mixing with R-parity violation, one has specific predictions for various branching ratios of the LSP decay as the structure of lepton flavor violating couplings is dictated by the pattern of the neutrino mixing. For this, it is of course necessary that the LSP has a short lifetime to produce a bunch of decay signals inside the detector. Since the total LSP decay rate is proportional to the (heaviest) neutrino mass, the measurement of the LSP decay length could also be useful to test the model. In the parameter space accommodating the neutrino data, we find that the LSP decay length is shorter than a few centimeters. The neutrino mixing angles are basically determined by the ratios of the introduced trilinear R-parity violating couplings. We will discuss how strong correlations they have and how the ratios of the couplings can be determined by measuring the LSP branching ratios. As we will see, the quite reliable information of the neutrino mixing angles can be drawn from the collider experiments if $\tan\beta$ is not too large. For large $\tan\beta$, the close correlations between the mixing angles and the trilinear couplings are lost because of the large tau Yukawa coupling effect.

This paper is organized as follows. In Sec. 2, we summarize how neutrino mass matrix can be generated up to 1-loop level in the context of mSUGRA with generic R-parity violating interactions. In the analysis, we take the basis where the bilinear R-parity term is rotated away. In Sec. 3, we make a qualitative analysis to examine the sizes of various R-parity violating couplings in mSUGRA which are required to account for the current neutrino oscillation data. In Sec. 4, we calculate the LSP decay rate and branching ratios of various modes and find how the model can be tested in the collider experiments. We will conclude in Sec. 5. Various useful formulae for the 1-loop contributions to the neutrino masses and sneutrino vacuum expectation values will be given in the appendices.

II. NEUTRINO MASS MATRIX AND FLAVOR STRUCTURE OF TRILINEAR COUPLINGS IN MSUGRA

Let us begin by writing the superpotential in the basis where the bilinear term $L_i H_2$ is rotated away :

$$W_0 = \mu H_1 H_2 + h_i^e L_i H_1 E_i^c + h_i^d Q_i H_1 D_i^c + h_i^u Q_i H_2 U_i^c, \tag{1}$$

$$W_1 = \lambda_i L_i L_3 E_3^c + \lambda_i' L_i Q_3 D_3^c, \tag{2}$$

where W_0 is R-parity conserving part and W_1 is R-parity violating part. Here, we have taken only 5 trilinear couplings, λ_i and λ_i', assuming the usual hierarchy of Yukawa couplings. Among soft SUSY breaking terms, R-parity violating bilinear terms are given by

$$V_0 = m^2_{L_i H_1} L_i H_1^\dagger + B_i L_i H_2 + h.c., \tag{3}$$

where B_i is the dimension-two soft parameter. We will denote the Higgs bilinear term as BH_1H_2. In the mSUGRA model, the bilinear parameters, $m^2_{L_iH_1}$ and B_i vanishes at the supersymmetry breaking mediation scale, and their non-zero values at the weak scale are generated through renormalization group evolution (RGE) which will be included in our numerical calculations. For the consistent calculation of the Higgs and slepton potential, we need to include the 1-loop contributions [10, 11] to the scalar potential as follows:

$$V_1 = \frac{1}{64\pi^2} \mathbf{Str} \mathcal{M}^4 \left(\ln \frac{\mathcal{M}^2}{Q^2} - \frac{3}{2} \right). \tag{4}$$

As is well-known, the electroweak symmetry breaking gives rise to a nontrivial vacuum expectation values of sneutrino (SVEV) $\tilde{\nu}_i$ as follows:

$$\xi_i \equiv \frac{\langle \tilde{\nu}_i \rangle}{\langle H_1^0 \rangle} = - \frac{m^2_{L_i H_1} + B_i t_\beta + \Sigma^{(1)}_{L_i}}{m^2_{\tilde{\nu}_i} + \Sigma^{(2)}_{L_i}}, \tag{5}$$

where the 1-loop contributions $\Sigma^{(1,2)}_{L_i}$ are given by $\Sigma^{(1)}_{L_i} = \partial V_1 / H_1^* \partial L_i$, $\Sigma^{(2)}_{L_i} = \partial V_1 / L_i^* \partial L_i$. Their explicit forms are presented in appendix B correcting various mistakes in the original calculation of Ref. [10]. The bilinear R-parity violating parameters induce the mixing between the ordinary particles and superparticles, namely, neutrinos/neutralinos, charged leptons/charginos, neutral Higgs bosons/sneutrinos, as well as charged Higgs bosons/charged sleptons. The mixing between neutrinos and neutralinos particularly serves as the origin of the tree-level neutrino masses. We note

that the parameters ξ_i should be very small to account for tiny neutrino masses. While the effect of such small parameters on the particle and sparticle mass spectra (apart from the neutrino sector) are negligible, they induce small but important R-parity violating vertices between the particles and sparticles, which in particular destabilizes the LSP together with the original trilinear couplings, λ_i and λ_i'. The derivation of the induced R-parity violating vertices has been presented in Ref. [7]. ¿From the seesaw formulae associated with the heavy four neutralinos, we obtain the light tree-level neutrino mass matrix of the form ;

$$M_{ij}^{tree} = -\frac{M_Z^2}{F_N}\xi_i\xi_j\cos^2\beta, \tag{6}$$

where $F_N = M_1M_2/M_{\tilde{\gamma}} + M_Z^2\cos 2\beta/\mu$ with $M_{\tilde{\gamma}} = c_W^2 M_1 + s_W^2 M_2$. The R-parity violating vertices between particles and sparticles can give rise to 1-loop neutrino masses. Including all the 1-loop corrections, the loop mass matrix can be written as [10]

$$M_{ij}^{loop} = -\frac{M_Z^2}{F_N}\left(\xi_i\delta_j + \delta_i\xi_j\right)\cos\beta + \Pi_{ij}, \tag{7}$$

where Π_{ij} denotes the 1-loop contribution of the neutrino self energy and

$$\begin{aligned} \delta_i &= \Pi_{\nu_i\widetilde{B}^0}\left(\frac{-M_2\sin^2\theta_W}{M_{\widetilde{\gamma}}M_W\tan\theta_W}\right) + \Pi_{\nu_i\widetilde{W}_3}\left(\frac{M_1\cos^2\theta_W}{M_{\widetilde{\gamma}}M_W}\right) \\ &+\Pi_{\nu_i\widetilde{H}_1^0}\left(\frac{\sin\beta}{\mu}\right) + \Pi_{\nu_i\widetilde{H}_2^0}\left(\frac{-\cos\beta}{\mu}\right). \end{aligned} \tag{8}$$

Analytic expressions of the 1-loop contributions $\Pi's$ are collected in Appendix A. Based on the neutrino mass matrix presented in the above, we will discuss whether the above mass matrix M^ν can account for both atmospheric and solar neutrino experimental data.

As we will see, the tree level neutrino masses are much larger than the 1-loop contributions, which makes it difficult to account for the solar and atmospheric neutrino oscillations. As a result, the observed ratio $\Delta m_{sol}^2/\Delta m_{amt}^2$ can be obtained in the mSUGRA only when some cancellation between the tree-level contributions to ξ_i occurs to make the tree-level neutrino masses comparable to the 1-loop contributions or even smaller than the 1-loop contributions.

III. NUMERICAL RESULTS: FITTING THE NEUTRINO DATA

Let us now examine how the parameters in mSUGRA can be constrained by the recent results from neutrino experiments. For our numerical analysis, we scan the input parameters in the following ranges;

$$\begin{aligned} 100\text{GeV} \leq\ & m_0 \leq 1000\text{GeV}, \\ 100\text{GeV} \leq\ & M_{1/2} \leq 1000\text{GeV}, \\ 0\text{GeV} \leq\ & A_0 \leq 700\text{GeV}, \\ 2 \leq\ & \tan\beta \leq 40. \end{aligned} \tag{9}$$

The ranges for $R-$parity violating parameters we scan are

$$\begin{aligned} 4\times10^{-6} \leq\ & |\lambda_1| \leq 6\times10^{-4}, \\ 4\times10^{-6} \leq\ & |\lambda_2| \leq 6\times10^{-4}, \\ 3\times10^{-9} \leq\ & \left|\lambda_1'\right| \leq 10^{-4}, \\ 4\times10^{-6} \leq\ & \left|\lambda_2'\right| \leq 10^{-3}, \\ 4\times10^{-6} \leq\ & \left|\lambda_3'\right| \leq 10^{-3}. \end{aligned} \tag{10}$$

We set the signs of $M_{1/2}$ and A_0 arbitrary, but find that most of the allowed parameter space corresponds to the case that both signs are positive.

A. General behavior of neutrino oscillation parameters

To understand the general feature of the R-parity violating mSUGRA model, we first plot the ratio $\Delta m^2_{sol}/\Delta m^2_{atm}$ for randomly generated points in the parameter space specified above. FIG. 1 shows that our model prefers the ratio in the range, $10^{-4} - 10^{-6}$, which implies the dominance of the tree-level mass over the loop mass. Only a small fraction of the points are within the allowed range denoted by two horizontal lines. The big dots in this range are the solution points accounting for the bi-large mixing of the solar and atmospheric neutrino oscillations, which can be basically arranged by appropriate choice of the R-parity violating couplings. We note that more solutions can be found for $\tan\beta \lesssim 15$. In FIG. 2, we plot $\sin^2 2\theta_{23}$ in terms of the ratios $|\xi_2/\xi_3|$ and $|\lambda'_2/\lambda'_3|$ showing the correlations between the atmospheric neutrino mixing angle and the ratios of the R-parity violating parameters. The figure shows that the parameter ξ_i has much cleaner correlation than λ'_i for the general points confirming the relation, $\sin^2 2\theta_{23} = 4|\xi_2|^2|\xi_3|^2/\sum_i |\xi_i|^2$ [5], which is a consequence of the tree mass dominance. An interesting observation is that λ'_i also maintains a rather clean correlation, which implies that λ'_i gives the larger contribution to ξ_i than λ_i. We also confirmed that the condition, $|\lambda'_i| < |\lambda'_2| \approx |\lambda'_3|$, is required to arrange the large atmospheric angle θ_{23} and the small CHOOZ angle θ_{13}.

B. Behavior of the solution points

In order to understand how the solution points can be obtained, we plot in FIG. 3, the quantity $|m_3^{loop} - m_3^{tree}|/m_3^{tree}$ for the loop corrected and tree-level mass eigenvalue m_3^{loop} and m_3^{tree}, respectively. In the general parameter space (a), the ratio is shown to be smaller than 0.1. The situation becomes quite different for the solution points (b), for which the loop mass is comparable to, or even larger than, the tree mass. This implies that there must be some cancellation in ξ_i to reduce the tree mass. As a result, the clean correlation between ξ_i and the angle θ_{23} is lost, which makes it difficult to probe neutrino oscillation through the LSP decays, as will be discussed later. In fact, λ'_i will have the better correlation than ξ_i for the solution points.

C. Importance of SVEV one-loop correction and neutral scalar loops

In FIG.4, we show how sizable the one-loop contributions to the SVEV are for the solution points. As can be seen from two figures, there occur almost order-one changes, which confirms cancellations in the tree-level values of ξ_i. This implies that the loop correction to the SVEV should be taken properly into account for the determination of the neutrino oscillation parameters in mSUGRA models.

It is also worthwhile to note that the the loop diagrams with virtual neutral scalars and neutralinos become sizable opposite to the case where the tree mass dominance works [7]. In order to see this, we consider the parameters defined by

$$\eta_i \equiv \xi_i - \frac{B_i}{B}, \tag{11}$$

which are relevant for the neutral scalar loops [13]. In the general parameter space, one finds η_i closely aligned with ξ_i so that the neutral scalar loops do not give important contributions. In FIG. 5, we plot $|(\xi_3-\eta_3)/\eta_3|$ vs. $|(\xi_2-\eta_2)/\eta_2|$ for the solution points. The results indicate that η_i can be much larger than ξ_i and more importantly the alignment between ξ_i and η_i is lost in generic points (which are away from the diagonal line). All of these observations make it complicated to understand the structure of the neutrino mass matrix from mSUGRA models. Namely, all the loop corrections have to be properly included in the determination of the neutrino oscillation parameters.

D. Fit to neutrino data

Now we are ready to present how the trilinear R-parity violating couplings are constrained by the mixing angles and mass-squared differences observed in the atmospheric and solar neutrino oscillations. In FIG. 6 and FIG. 7, we show the correlations between the atmospheric neutrino mixing angle and the ratios ξ_2/ξ_3 and λ'_2/λ'_3, respectively. As indicated before, we find a better correlation with the latter. Even though λ'_2/λ'_3 has no analytic relation with θ_{23} for the solution points, we can obtain the following favorable ranges through the parameter scan: $|\lambda'_2/\lambda'_3|$ from the neutrino data

$$0.4 \lesssim |\lambda'_2/\lambda'_3| \lesssim 2.5 \ \text{ for } \ \tan\beta = 3 - 15$$

$$0.3 \lesssim |\lambda'_2/\lambda'_3| \lesssim 3.3 \ \text{ for } \ \tan\beta = 30 - 40. \tag{12}$$

It is also amusing to find the correlation between the ratio λ_2/λ_3 and the solar neutrino mixing angle θ_{12} as shown in FIG. 8. Similar to the case of the atmospheric neutrino oscillation, we can get the constraints:

$$\begin{aligned} 0.3 \lesssim |\lambda_1/\lambda_2| \lesssim 1.6 \ \text{ for } \ \tan\beta = 3 - 15, \\ 0.2 \lesssim |\lambda_1/\lambda_2| \lesssim 5.0 \ \text{ for } \ \tan\beta = 30 - 40. \end{aligned} \tag{13}$$

In addition, fitting the measured mass-squared values, we find the allowed regions as follows:

$$|\lambda_{1,2}|\,, \ |\lambda'_{2,3}| \ = \ (0.1 - 2) \times 10^{-4}, \tag{14}$$

$$|\lambda'_1| \ < \ 2.5 \times 10^{-5}. \tag{15}$$

Eqs. (12)-(15) are the key prediction of the mSUGRA model, some of which can be tested in the future colliders.

IV. COLLIDER TEST OF THE MODEL

In this section, we will investigate how the mSUGRA scenario for the neutrino masses and mixing can be tested in the collider experiments. Since the LSP is destabilized by the R-parity violating interactions, the structure of the R-parity violating couplings drawn in the above section may be probed by observing the lepton number violating signals of the LSP decay. Based on the parameter sets constrained by the neutrino data, we first determine the type of the LSP, which can be either a neutralino or a stau. Then, we calculate the cross section for the pair production of the LSP, and then its decay length and branching ratios. To consider the observability of the various decay modes, we will take the luminosity 1000/fb/yr in the next linear colliders [14, 15]. For our presentation, we will show the trilinear R-parity violating parameters and the resulting neutrino oscillation parameters by selecting some typical examples of solution points and then give predictions of the production cross section and the decay length with important branching ratios of the LSP. As will be shown later, the LSP production cross sections are of the order 10-100 fb so that the branching ratios of the order $10^{-4} - 10^{-3}$ will be measurable in the planned linear colliders.

A. Stau LSP

When the LSP is the stau, $\tilde{\tau}_1$, it mainly decays into two leptons through the coupling λ_i. For small $\tan\beta$, $\tilde{\tau}_1$ is almost the right-handed stau $\tilde{\tau}_R$ due to the small left-right mixing mass. Then the light stau almost decays into leptons via $\lambda_i L_i L_3 E_3^c$ terms in the superpotential. Thus, one can expect that the branching ratios of those decay channels depend on the parameter λ_i. In this case, the following relation holds,

$$Br(e\nu) : Br(\mu\nu) : Br(\tau\nu) \simeq |\lambda_1|^2 : |\lambda_2|^2 : |\lambda_1|^2 + |\lambda_2|^2, \tag{16}$$

as can be seen from Table I. Note that the decay length is much smaller than micro-meter(μm) so that the stau LSP production and decay occur instantaneously. The R-parity violating signals in the linear collider will be

$$e^+e^- \to \tilde{\tau}_1\bar{\tilde{\tau}}_1 \to l_i^+ l_j^- \nu\bar{\nu}$$

, which are identical to the Standard Model background,

$$e^+e^- \to W^+W^- \to l_i^+ l_j^- \nu\bar{\nu}\,.$$

But this is a flavor independent process and can be deduced from the total number of events to establish the flavor dependent quantities $Br(l_i\nu)$. Therefore, the observation of the following relations:

$$\begin{aligned} Br(\tau\nu) \ &= \ Br(e\nu) + Br(\mu\nu), \\ \frac{Br(e\nu)}{Br(\mu\nu)} \ &\approx \ 0.1 - 2.6. \end{aligned} \tag{17}$$

will be a strong indication of the R-parity violation predicting Eqs. (17) and (14).

The situation is more complicated for large $\tan\beta$. A characteristic feature of this case is that there is a sizable fraction of the stau LSP decay into top and bottom quarks, if available kinematically, which is a consequence of a

large left-right stau mixing. However, the above relation (16) becomes obscured by the large tau Yukawa coupling effect. In TABLE II, we show this behavior for $\tan\beta = 38$. One can see that the ratio of the branching ratios, $Br(e\nu) : Br(\mu\nu) : Br(\tau\nu) \simeq 11.5 : 25.5 : 47.2$, deviates from the λ_i coupling ratio, $|\lambda_1|^2 : |\lambda_2|^2 : |\lambda_1|^2 + |\lambda_2|^2 \simeq 15.6 : 34.4 : 50.0$. The deviation from the relation (17) comes from the large mixing between the stau and the charged Higgs. Another effect would be the charged Higgs contribution to the event:

$$e^+e^- \to H^+H^- \to \tau^+\tau^-\nu\bar{\nu}\,.$$

Even though a clean prediction for the τ sector is lost, we are still able to establish the lepton number violating signals in the first two generations and measure the quantity:

$$\frac{Br(e\nu)}{Br(\mu\nu)} = \left|\frac{\lambda_1}{\lambda_2}\right|^2 \approx 0.04 - 25\,. \tag{18}$$

B. Neutralino LSP

The lepton number violating signatures from the neutralino decay have been studied extensively as the LSP is a neutralino in the most parameter space [4, 5, 6, 7]. A characteristic feature of the neutralino LSP is that the vertex for the process $\tilde{\chi}^0_1 \to l_i W$ is proportional to ξ_i which determines the tree-level neutrino mass (6). As a result, measuring the branching ratios $Br(l_i jj)$ through either on-shell or off-shell W bosons will determine the ratio of $|\xi_i|^2$, that is,

$$Br(ejj) : Br(\mu jj) : Br(\tau jj) = |\xi_1|^2 : |\xi_2|^2 : |\xi_3|^2. \tag{19}$$

If the tree mass dominates over the loop mass, which is usually the case in the gauge-mediated supersymmetry breaking models [7], the neutrino mixing angles θ_{23} and θ_{13} can be cleanly measured in colliders [5]. Unfortunately, this is not the case in the mSUGRA model under consideration. As we discussed in the previous section (See Fig. 3), the tree mass has to be suppressed and thus the variables ξ_i are not correlated with the mixing angles θ_{23} and θ_{13} in general and λ'_i maintain better correlations (See Fig. 6 and 7). ¿From Tables III-VI, one can see that $Br(l_i jj)$ or $Br(l_i W)$ are proportional to ξ_i^2 which, however, lost the correlation with the mixing angles.

On the other hand, similarly to the stau LSP case, we can extract the information on λ_i from the measurement of $\nu l_i^\pm \tau^\mp$ branching ratios for small $\tan\beta$ because the following relation,

$$Br(\nu e^\pm\tau^\mp) : Br(\nu\mu^\pm\tau^\mp) : Br(\nu\tau^\pm\tau^\mp) \simeq |\lambda_1|^2 : |\lambda_2|^2 : |\lambda_1|^2 + |\lambda_2|^2, \tag{20}$$

holds as shown in Tables III-VI. Likewise, if we measure the above branching ratios, the models can be tested by comparing them with the values allowed by the neutrino experimental data as in Eq. (18). Note that this is the case for small $\tan\beta < 15$. For large $\tan\beta$, the relation (21) is invalidated again because of the large tau Yukawa coupling effect.

Another interesting aspect is that the parameters λ'_i can be probed *if the neutralino LSP is heavy enough to allow the decay modes,* $l_i t\bar{b}$. The main contributions to these final states come from the couplings λ'_i and thus one obtains the following approximate relation:

$$Br(et\bar{b}) : Br(\mu t\bar{b}) : Br(\tau t\bar{b}) \approx |\lambda'_1|^2 : |\lambda'_2|^2 : |\lambda'_3|^2 \tag{21}$$

which should be consistent with the predictions (12), (14) and (15). In Table V, one finds the branching ratios for $l_i t\bar{b}$ large enough to be measured in the colliders with the integrated luminosity of 1000/fb. The branching ratios get too small if the LSP mass is more than twice top quark mass as shown in Table VI. This is because the $\nu t\bar{t}$ mode occurring through the light Higgs exchange becomes dominating.

V. CONCLUSION

We have investigated the neutrino masses and mixing originated from the R-parity violation and its possible collider test in the context of the minimal supergravity model (mSUGRA) where the soft terms are assumed to be universal at the ultraviolet scale. In this scheme, the bi-large mixing accounting for the atmospheric and solar neutrino data can be obtained by allowing five independent tri-linear couplings, λ_i and λ'_i. In the mSUGRA model, the tree-level contribution to the neutrino mass matrix is too much large compared with the one-loop contribution in the generic parameter space. In order to obtain the observed value of $\Delta m^2_{sol}/\Delta m^2_{atm}$, the parameters needs to be tuned to arrange

some cancellation in the tree-level mass which is made to be comparable to the loop mass. As a result, a nice relation between the R-parity (and lepton number) violating parameters and the neutrino oscillation parameters is lost. This is a dis-favorable feature of the mSUGRA model with R-parity violation as the origin of the observed neutrino mass matrix. However, in the allowed region of the parameter space, we still find the reasonable correlations between the tri-linear R-parity violating couplings and the neutrino mixing angles. That is, the bi-large mixing of the atmospheric and solar neutrino oscillation requires $|\lambda'_2| \sim |\lambda'_3|$ (12) and $|\lambda_1| \sim |\lambda_2|$ (13), while the small mixing angle θ_{13} requires $|\lambda'_1| \ll |\lambda'_{2,3}|$ (15).

Such correlations predict some distinctive lepton flavor violating signatures of the LSP decay in the next linear colliders, which can provide a test for the R-parity violation scenario. If the stau is the LSP, there is no way to probe the couplings λ'_i and thus the two mixing angles θ_{23} and θ_{13}. However, it is still possible to obtain the information on the solar neutrino mixing angle θ_{12} since the stau decays into the final states $l_i\nu$ through the couplings λ_i. When $\tan\beta$ is not too large, the relation $Br(e\nu) : Br(\mu\nu) : Br(\tau\nu) = |\lambda_1|^2 : |\lambda_2|^2 : |\lambda_1|^2 + |\lambda_2|^2$ can be checked to confirm or disprove our scenario. For large $\tan\beta$, the last relation in the τ sector is obscured by the large tau Yukawa coupling effect. Thus, it will not be possible to establish the above relation without knowing other parameters like $\tan\beta$, Higgs masses, etc. For the case of the neutralino LSP, its decay into $\nu l_i^\pm \tau^\mp$ can be observed to establish the similar relation as above: $Br(\nu e^\pm\tau^\mp) : Br(\nu\mu^\pm\tau^\mp) : Br(\nu\tau^\pm\tau^\mp) = |\lambda_1|^2 : |\lambda_2|^2 : |\lambda_1|^2 + |\lambda_2|^2$. Again, such a clean relation is invalidated in the τ sector for large $\tan\beta$. If the neutralino is heavier the top quark, it can decay into $l_i t\bar{b}$ through the couplings λ'_i, predicting $Br(et\bar{b}) : Br(\mu t\bar{b}) : Br(\tau t\bar{b}) \approx |\lambda'_1|^2 : |\lambda'_2|^2 : |\lambda'_3|^2$. Thus, its measurement can provide information on the atmospheric neutrino mixing angle. Let us note that such simple correlations are valid only for small $\tan\beta \lesssim 15$.

Acknowledgments

This work was supported by the Korea Research Foundation Grant, KRF-2002-015-CP0060, EJC was supported by KRF-2002-070-C00022, and SKK by BK21 program of the Minstry of Education.

APPENDIX A

In the appendix A, we present the explicit forms of 1-loop contributions Π's. Let us begin by fixing the notations for the diagonalization of the mass matrices. The mixing between the standard model particles and the supersymmetric ones in the R-parity violating model can be rotated away via the so-called seesaw diagonalization which makes the mass matrices block-diagonal, and then each blocks can separately be diagonalized.

Neutrino-neutralino diagonalization

The neutrinos/neutralinos mass matrix is written in 7×7 form as,

$$\mathcal{M}_{\mathbf{N}} = \begin{pmatrix} 0 & M_{\nu N} \\ M_{\nu N}^\dagger & M_N \end{pmatrix}, \tag{A.1}$$

in the bases $(\nu_e, \nu_\mu, \nu_\tau, \tilde{B}, \tilde{W}_3, \tilde{H}_1^0, \tilde{H}_2^0)$. Rotating away the neutrino-neutralino mixing mass terms can be made by the following redefinition of neutrinos and neutralinos with θ^N

$$\begin{pmatrix} \nu_i \\ \chi_j^0 \end{pmatrix} \longrightarrow \begin{pmatrix} \nu_i - \theta_{ik}^N \chi_k^0 \\ \chi_j^0 + \theta_{lj}^N \nu_l \end{pmatrix}, \tag{A.2}$$

where (ν_i) and (χ_j^0) represent three neutrinos $(\nu_e, \nu_\mu, \nu_\tau)$ and four neutralinos $(\tilde{B}, \tilde{W}_3, \tilde{H}_1^0, \tilde{H}_2^0)$ in the flavor basis, respectively. The rotation parameters θ_{ij}^N are given by

$$\begin{aligned} \theta_{ij}^N &= \xi_i c_j^N c_\beta - \epsilon_i \delta_{j3}, \\ (c_j^N) &= \frac{M_Z}{F_N}\left(\frac{s_W M_2}{c_W^2 M_1 + s_W^2 M_2}, -\frac{c_W M_1}{c_W^2 M_1 + s_W^2 M_2}, -s_\beta \frac{M_Z}{\mu}, c_\beta \frac{M_Z}{\mu} \right). \end{aligned} \tag{A.3}$$

where $F_N = M_1 M_2/(c_W^2 M_1 + s_W^2 M_2) + M_Z^2 s_{2\beta}/\mu$. Here $s_W = \sin\theta_W$ and $c_W = \cos\theta_W$ with the weak mixing angle θ_W. After rotating away the mixing terms, the mass matrix has block-diagonal form with 3×3 neutrino mass matrix

M_ν and 4×4 neutralino mass matrix in each blocks. In particular, the neutralino mass matrix is diagonalized by 4×4 mixing matrix N,

$$N^\dagger M_N N = (M_N)_{diag}. \tag{A.4}$$

Charged lepton/chargino diagonalization

SImilar to the above case, charged leptons are also get mixed with charginos. Then the 5×5 matrix is written as

$$\mathcal{M}_{\mathbf{C}} = \left(\begin{array}{cc} M_{ll} & M_{l\tilde{\chi}^\pm} \\ M_{\tilde{\chi}^\pm l} & M_{\tilde{\chi}^\pm\tilde{\chi}^\pm} \end{array}\right), \tag{A.5}$$

in the bases $\left(e_i, \widetilde{W}^-, \widetilde{H}_1^-\right)$, $\left(e_i^c, \widetilde{W}^+, \widetilde{H}_1^+\right)$. Defining θ^L and θ^R as the two rotation matrices corresponding to the left-handed negatively and positively charged fermions, we have

$$\left(\begin{array}{c} e_i \\ \chi_j^- \end{array}\right) \to \left(\begin{array}{c} e_i - \theta^L_{ik}\chi_k^- \\ \chi_j^- + \theta^L_{lj} e_l \end{array}\right) \quad ; \quad \left(\begin{array}{c} e_i^c \\ \chi_j^+ \end{array}\right) \to \left(\begin{array}{c} e_i^c - \theta^R_{ik}\chi_k^+ \\ \chi_j^+ + \theta^R_{lj} e_l^c \end{array}\right), \tag{A.6}$$

where e_i and e_i^c denote the left-handed charged leptons and anti-leptons, $(\chi_j^-) = (\tilde{W}^-, \tilde{H}_1^-)$ and $(\chi_j^+) = (\tilde{W}^+, \tilde{H}_2^+)$. The rotation parameters $\theta^{L,R}_{ij}$ are given by

$$\begin{aligned}
&\theta^L_{ij} = \xi_i c^L_j c_\beta - \epsilon_i \delta_{j2}\ , \quad \theta^R_{ij} = \frac{m_i^e}{F_C}\xi_i c^R_j c_\beta \quad \text{and} \\
&(c^L_j) = -\frac{M_W}{F_C}(\sqrt{2}, 2s_\beta \frac{M_W}{\mu})\ , \\
&(c^R_j) = -\frac{M_W}{F_C}(\sqrt{2}(1-\frac{M_2}{\mu}t_\beta), \frac{M_2^2 c_\beta^{-1}}{\mu M_W} + 2\frac{M_W}{\mu}c_\beta),
\end{aligned} \tag{A.7}$$

and $F_C = M_2 + M_W^2 s_{2\beta}/\mu$. After block diagonalizing, the 2×2 chargino mass matrix $M_{\tilde{\chi}^\pm\tilde{\chi}^\pm}$ is diagonalized

$$V^\dagger M_{\tilde{\chi}^\pm\tilde{\chi}^\pm} U = (M_{\tilde{\chi}^\pm\tilde{\chi}^\pm})_{diag}. \tag{A.8}$$

Sneutrino/neutral Higgs boson diagonalization

Denoting the rotation matrix by θ^S, we get

$$\left(\begin{array}{c} \tilde{\nu}_i \\ H_1^0 \\ H_2^0 \end{array}\right) \to \left(\begin{array}{c} \tilde{\nu}_i - \theta^S_{i1}H_1^0 - \theta^S_{i2}H_2^{0*} - \theta^S_{i3}H_1^{0*} - \theta^S_{i4}H_2^0 \\ H_1^0 + \theta^S_{i1}\tilde{\nu}_i + \theta^S_{i3}\tilde{\nu}_i^* \\ H_2^0 + \theta^S_{i2}\tilde{\nu}_i^* + \theta^S_{i4}\tilde{\nu}_i \end{array}\right), \tag{A.9}$$

where

$$\begin{aligned}
\theta^S_{i1} &= -\xi_i - \eta_i s_\beta^2 m_A^2 [m_{\tilde{\nu}_i}^4 - m_{\tilde{\nu}_i}^2(m_A^2 + M_Z^2 s_\beta^2) - m_A^2 M_Z^2 s_\beta^2 c_{2\beta}]/F_S, \\
\theta^S_{i2} &= +\eta_i s_\beta c_\beta m_A^2 [m_{\tilde{\nu}_i}^4 - m_{\tilde{\nu}_i}^2(m_A^2 + M_Z^2 c_\beta^2) + m_A^2 M_Z^2 c_\beta^2 c_{2\beta}]/F_S, \\
\theta^S_{i3} &= -\eta_i s_\beta^2 c_\beta^2 m_A^2 M_Z^2 [m_{\tilde{\nu}_i}^2 - m_A^2 c_{2\beta}]/F_S, \\
\theta^S_{i3} &= +\eta_i s_\beta^3 c_\beta m_A^2 M_Z^2 [m_{\tilde{\nu}_i}^2 + m_A^2 c_{2\beta}]/F_S,
\end{aligned} \tag{A.10}$$

with $F_S = (m_{\tilde{\nu}_i}^2 - m_h^2)(m_{\tilde{\nu}_i}^2 - m_H^2)(m_{\tilde{\nu}_i}^2 - m_A^2)$ and m_A, m_h and m_H are the masses of pseudo-scalar, light and heavy neutral scalar Higgs bosons, respectively. Note that $m_A^2 = -B\mu/c_\beta s_\beta$ in our convention. For our calculation, we assume that all the R-parity violating parameters are real and thus all θ's are real, too. We also note that the presence of the scalar fields as well as their complex conjugates in Eq. (A.9) is due to the electroweak symmetry breaking, which is expected to be suppressed with M_Z^2. Sneutrino and Higgs mass matrices can then separately be

diagonalized.

Charged slepton/charged Higgs boson diagonalization

Defining θ^C as the rotation matrix, we have

$$\begin{pmatrix} \tilde{e}_i \\ \tilde{e}_i^{c*} \\ H_1^- \\ H_2^- \end{pmatrix} \rightarrow \begin{pmatrix} \tilde{e}_i - \theta^C_{i1} H_1^- - \theta^C_{i2} H_2^- \\ \tilde{e}_i^{c*} - \theta^C_{i3} H_1^- - \theta^C_{i4} H_2^- \\ H_1^- + \theta^C_{i1}\tilde{e}_i + \theta^C_{i3}\tilde{e}_i^{c*} \\ H_2^- + \theta^C_{i2}\tilde{e}_i + \theta^C_{i4}\tilde{e}_i^{c*} \end{pmatrix}, \tag{A.11}$$

where

$$\begin{aligned}
\theta^C_{i1} &= -\xi_i - \eta_i \frac{s_\beta^2 m_A^2 (m_{Ri}^2 - m_{H^-}^2)}{(m_{H^-}^2 - m_{\tilde{e}_{i1}}^2)(m_{H^-}^2 - m_{\tilde{e}_{i2}}^2)} - \xi_i \frac{m_i^e \mu m_{Di}^2 t_\beta}{(m_{H^-}^2 - m_{\tilde{e}_{i1}}^2)(m_{H^-}^2 - m_{\tilde{e}_{i2}}^2)}, \\
\theta^C_{i2} &= -\eta_i \frac{s_\beta c_\beta m_A^2 (m_{Ri}^2 - m_{H^-}^2)}{(m_{H^-}^2 - m_{\tilde{e}_{i1}}^2)(m_{H^-}^2 - m_{\tilde{e}_{i2}}^2)} - \xi_i \frac{m_i^e \mu m_{Di}^2}{(m_{H^-}^2 - m_{\tilde{e}_{i1}}^2)(m_{H^-}^2 - m_{\tilde{e}_{i2}}^2)}, \\
\theta^C_{i3} &= +\eta_i \frac{s_\beta^2 m_A^2 m_{Di}^2}{(m_{H^-}^2 - m_{\tilde{e}_{i1}}^2)(m_{H^-}^2 - m_{\tilde{e}_{i2}}^2)} + \xi_i \frac{m_i^e \mu m_{Li}^2 (m_{Li}^2 - m_{H^-}^2) t_\beta}{(m_{H^-}^2 - m_{\tilde{e}_{i1}}^2)(m_{H^-}^2 - m_{\tilde{e}_{i2}}^2)}, \\
\theta^C_{i4} &= +\eta_i \frac{s_\beta c_\beta m_A^2 m_{Di}^2}{(m_{H^-}^2 - m_{\tilde{e}_{i1}}^2)(m_{H^-}^2 - m_{\tilde{e}_{i2}}^2)} + \xi_i \frac{m_i^e \mu (m_{Li}^2 - m_{H^-}^2)}{(m_{H^-}^2 - m_{\tilde{e}_{i1}}^2)(m_{H^-}^2 - m_{\tilde{e}_{i2}}^2)}.
\end{aligned} \tag{A.12}$$

Here, m_{H^-} stands for the charged-Higgs boson mass, and m_{Li}^2, m_{Ri}^2 and m_{Di}^2 correspond to the LL, RR and LR components of the i-th charged-slepton mass-squared matrix, respectively, and $m_{\tilde{e}_{i1,i2}}^2$ are their eigenvalues. We remark that the appearance of ξ_i in θ^S_{i1} and θ^C_{i1} is due to the fact that we performed the rotation to remove the Goldstone mode from the redefined sneutrino fields.

With the above notations, let us present the 1-loop contributions Π's:

$$\begin{aligned}
\Pi_{ij} = &- \frac{g^2}{32\pi^2}(t_W N_{1a} - N_{2a})^2 m_{\tilde{\chi}^0_a} \mathbf{F^a_{ij}} \\
&+ \Big\{ \frac{g h_\tau}{16\pi^2}\delta_{i3}\left[\theta^R_{3m} U_{1a} V_{ma} m_{\tilde{\chi}^0_a} \mathbf{K^a_{1j}} - \theta^L_{34} m_\tau \mathbf{K^\tau_{1j}}\right] \\
&\quad + \frac{g\lambda_i}{16\pi^2}\delta_{j3}\left[\theta^R_{3m} U_{1a} V_{ma} m_{\tilde{\chi}^-_a} \mathbf{E0^a_3} - \theta^L_{34} m_\tau \mathbf{E0^\tau_3}\right] \\
&\quad + \frac{g\lambda_i}{16\pi^2}\delta_{j3}\left[-\theta^R_{3m} U_{1a} V_{ma} m_{\tilde{\chi}^-_a} \mathbf{E0^a_i} + \theta^L_{34} m_\tau \mathbf{E0^\tau_i}\right] \\
&\quad + \frac{h_\tau^2}{16\pi^2}\delta_{i3}\delta_{j3}\left[\theta^R_{3m} U_{2a} V_{ma} m_{\tilde{\chi}^-_a} \mathbf{Q^a_{1i}} - \theta^L_{35} m_\tau \mathbf{Q^\tau_{1i}}\right] \\
&\quad + \frac{h_i\lambda_j}{16\pi^2}\delta_{i3}\left[\theta^R_{3m} U_{2a} V_{ma} m_{\tilde{\chi}^-_a} \mathbf{H0^a_3} - m_\tau \mathbf{Q^\tau_{13}}\right] \\
&\quad - \frac{\lambda_i\lambda_j}{16\pi^2} m_\tau \mathbf{H0^\tau_3} \\
&\quad - \frac{\lambda'_i\lambda'_j}{16\pi^2} m_b \mathbf{P_{\tilde{b}\tilde{b}^c}} \\
&\quad + (i \longleftrightarrow j) \Big\},
\end{aligned} \tag{A.13}$$

$$\begin{aligned}
\Pi_{i\tilde{B}} = &- \frac{g^2}{32\pi^2}(t_W N_{1a} - N_{2a})[\, t_W N_{3a} m_{\tilde{\chi}^0_a} \mathbf{G^a_{1i}} - t_W N_{4a} m_{\tilde{\chi}^0_a} \mathbf{G^a_{2i}}\,] \\
&- \frac{g^2}{16\pi^2}\frac{t_W}{\sqrt{2}}[\, U_{1a} V_{2a} m_{\tilde{\chi}^-_a} \mathbf{K^a_{2i}} - 2\theta^R_{im} U_{1a} V_{ma} m_{\tilde{\chi}^-_a} \mathbf{H0^a_i} - \delta_{i3} 2\theta^L_{34} m_\tau \mathbf{H0^\tau_3}\,] \\
&- \frac{h_i g}{16\pi^2}\frac{t_W}{\sqrt{2}}[\quad U_{2a} V_{2a} m_{\tilde{\chi}^-_a} \mathbf{Q^a_{2i}} - 2\theta^R_{im} U_{2a} V_{ma} m_{\tilde{\chi}^-_a} \mathbf{C0^a_i}
\end{aligned}$$

$$
\begin{aligned}
& \qquad\qquad + \theta^R_{im} V_{ma} U_{2a} m_{\tilde\chi^-_a} \mathbf{J^a} - \delta_{i3}\theta^L_{32} m_\tau \mathbf{J}^\tau - \delta_{i3}\delta_{j3} m_\tau \mathbf{K^\tau_{ij}} \,] \\
& - \frac{\lambda_i g}{16\pi^2}\frac{t_W}{\sqrt{2}}[\, 2m_\tau \mathbf{C0^\tau_3} - m_\tau \mathbf{E0^\tau_3} \,] \\
& - \frac{\lambda'_i}{16\pi^2}\frac{t_W}{3\sqrt{2}}[\, 2m_b \mathbf{P_{\tilde b^c \tilde b^{c*}}} + m_b \mathbf{P_{\tilde b \tilde b^*}} \,],
\end{aligned}
\tag{A.14}
$$

$$
\begin{aligned}
\Pi_{i\tilde W^3} = & - \frac{g^2}{32\pi^2}(t_W N_{1a} - N_{2a})[\, -N_{3a} m_{\tilde\chi^0_a} \mathbf{G^a_{1i}} + N_{4a} m_{\tilde\chi^0_a} \mathbf{G^a_{2i}} \,] \\
& - \frac{g^2}{16\pi^2}\frac{1}{\sqrt{2}} U_{1a} V_{2a} m_{\tilde\chi^-_a} \mathbf{K^a_{2i}} \\
& + \frac{h_i g}{16\pi^2}\frac{1}{\sqrt{2}}[\, U_{2a} V_{2a} m_{\tilde\chi^-_a} \mathbf{Q^a_{2i}} + \theta^R_{im} V_{ma} U_{2a} m_{\tilde\chi^-_a} \mathbf{J^a} \\
& \qquad - \delta_{i3}\theta^L_{32} m_\tau \mathbf{J}^\tau - \delta_{i3}\delta_{j3} m_\tau \mathbf{K^\tau_{1j}} \,] \\
& + \frac{\lambda_i g}{16\pi^2}\frac{1}{\sqrt{2}} m_\tau \mathbf{E0^\tau_3} \\
& + \frac{\lambda'_i g}{16\pi^2}\frac{1}{\sqrt{2}} m_b \mathbf{P_{\tilde b \tilde b^*}},
\end{aligned}
\tag{A.15}
$$

$$
\begin{aligned}
\Pi_{i\tilde H_1} = & - \frac{g^2}{32\pi^2}(t_W N_{1a} - N_{2a})^2 m_{\tilde\chi^0_a} \mathbf{G^a_{1i}} \\
& - \frac{g h_i}{16\pi^2}[\, \theta^R_{im} U_{1a} V_{ma} m_{\tilde\chi^-_a} \mathbf{E0^a_i} - \theta^R_{im} V_{ma} U_{1a} m_{\tilde\chi^-_a} \mathbf{J^a} \\
& \qquad + \delta_{i3}\theta^L_{31} m_\tau \mathbf{J}^\tau - \delta_{i3}\theta^L_{31} m_\tau \mathbf{E0^\tau_i} \,] \\
& - \frac{h_i^2}{16\pi^2}\theta^R_{im} U_{2a} V_{ma} m_{\tilde\chi^-_a} \mathbf{H0^a_i} \\
& + \frac{h_i h_\tau}{16\pi^2}[\, \delta_{i3}\theta^L_{32} m_\tau \mathbf{H0^\tau_3} + \delta_{i3} m_\tau \mathbf{Q^\tau_{1k}} \delta_{k3} \,] \\
& + \frac{\lambda_i h_\tau}{16\pi^2} 2m_\tau \mathbf{H0^\tau_3} \\
& + \frac{\lambda'_i h_b}{16\pi^2} 2m_b \mathbf{P_{\tilde b \tilde b^c}},
\end{aligned}
\tag{A.16}
$$

$$
\begin{aligned}
\Pi_{i\tilde H_2} = & \;\; \frac{g^2}{32\pi^2}(t_W N_{1a} - N_{2a})^2 m_{\tilde\chi^0_a} \mathbf{G^a_{2i}} \\
& - \frac{g^2}{16\pi^2} U_{1a} V_{1a} m_{\tilde\chi^-_a} \mathbf{K^a_{2i}} \\
& - \frac{h_i g}{16\pi^2} U_{2a} V_{1a} m_{\tilde\chi^-_a} \mathbf{Q^a_{2i}},
\end{aligned}
\tag{A.17}
$$

where the functions defined above are

$$
\begin{aligned}
\mathbf{F^a_{ij}} &= \frac{1}{2}\delta_{ij}\left[B_0(m^2_{\chi^0_a}, m^2_{\tilde\nu_i{}^R}) - B_0(m^2_{\chi^0_a}, m^2_{\tilde\nu_i{}^I})\right] \\
& \quad + Z_{ji} B_0(m^2_{\tilde\chi^0_a}, m^2_{\tilde\nu_i}) + Z_{ij} B_0(m^2_{\tilde\chi^0_a}, m^2_{\tilde\nu_i}) \\
& \quad + \frac{1}{2}\theta_{ih}\theta_{jh} B_0(m^2_{\tilde\chi^0_a}, m^2_h) + \frac{1}{2}\theta_{iH}\theta_{jH} B_0(m^2_{\tilde\chi^0_a}, m^2_H) \\
& \quad - \frac{1}{2}\theta_{iA}\theta_{jA} B_0(m^2_{\tilde\chi^0_a}, m^2_A), \\
\mathbf{G^a_{1i}} &= \theta^S_{i3} B_0(m^2_{\tilde\chi^0_a}, m^2_{\tilde\nu_i}) + \frac{1}{2}s_\alpha\theta_{ih} B_0(m^2_{\tilde\chi^0_a}, m^2_h) \\
& \quad - \frac{1}{2}c_\alpha\theta_{iH} B_0(m^2_{\tilde\chi^0_a}, m^2_H) + \frac{1}{2}s_\beta\theta_{iA} B_0(m^2_{\tilde\chi^0_a}, m^2_A), \\
\mathbf{G^a_{2i}} &= \theta^S_{i2} B_0(m^2_{\tilde\chi^0_a}, m^2_{\tilde\nu_i}) - \frac{1}{2}c_\alpha\theta_{ih} B_0(m^2_{\tilde\chi^0_a}, m^2_h) \\
& \quad - \frac{1}{2}s_\alpha\theta_{iH} B_0(m^2_{\tilde\chi^0_a}, m^2_H) + \frac{1}{2}s_\beta\theta_{iA} B_0(m^2_{\tilde\chi^0_a}, m^2_A),
\end{aligned}
$$

$$
\begin{aligned}
\mathbf{E^a_{ij}} &= \delta_{ij}\left[c_i^2 B_0(m^2_{\tilde\chi^-_a}, m^2_{\tilde e_{i1}}) + s_i^2 B_0(m^2_{\tilde\chi^-_a}, m^2_{\tilde e_{i2}})\right] \\
&\quad + \left(\theta^C_{i1}\theta^C_{j1}s^2_\beta + \theta^C_{i1}\theta^C_{j2}s_\beta c_\beta + \theta^C_{i2}\theta^C_{j1}c_\beta s_\beta + \theta^C_{i2}\theta^C_{j2}c^2_\beta\right) B_0(m^2_{\tilde\chi^-_a}, m^2_{H^-}), \\
\mathbf{H^a_{ij}} &= -\delta_{ij}c_i s_i\left[B_0(m^2_{\tilde\chi^-_a}, m^2_{\tilde e_{i1}}) - B_0(m^2_{\tilde\chi^-_a}, m^2_{\tilde e_{i1}})\right] \\
&\quad + \left(\theta^C_{i1}\theta^C_{j3}s^2_\beta + \theta^C_{i1}\theta^C_{j4}s_\beta c_\beta + \theta^C_{i2}\theta^C_{j3}c_\beta s_\beta + \theta^C_{i2}\theta^C_{j4}c^2_\beta\right) B_0(m^2_{\tilde\chi^-_a}, m^2_{H^-}), \\
\mathbf{K^a_{1i}} &= \left(\theta^C_{i1}c_i^2 - \theta^C_{i3}c_i s_i\right) B_0(m^2_{\tilde\chi^-_a}, m^2_{\tilde e_{i1}}) + \left(\theta^C_{i1}s_i^2 + \theta^C_{i3}c_i s_i\right) B_0(m^2_{\tilde\chi^-_a}, m^2_{\tilde e_{i2}}) \\
&\quad - \left(\theta^C_{i1}s^2_\beta + \theta^C_{i2}c_\beta s_\beta\right) B_0(m^2_{\tilde\chi^-_a}, m^2_{H^-}), \\
\mathbf{K^a_{2i}} &= \left(\theta^C_{i2}c_i^2 - \theta^C_{i4}c_i s_i\right) B_0(m^2_{\tilde\chi^-_a}, m^2_{\tilde e_{i1}}) + \left(\theta^C_{i2}s_i^2 + \theta^C_{i4}c_i s_i\right) B_0(m^2_{\tilde\chi^-_a}, m^2_{\tilde e_{i2}}) \\
&\quad - \left(\theta^C_{i1}s_\beta c_\beta + \theta^C_{i2}c^2_\beta\right) B_0(m^2_{\tilde\chi^-_a}, m^2_{H^-}), \\
\mathbf{Q^a_{1i}} &= \left(-\theta^C_{i1}c_i s_i + \theta^C_{i3}s_i^2\right) B_0(m^2_{\tilde\chi^-_a}, m^2_{\tilde e_{i1}}) + \left(\theta^C_{i1}s_i c_i + \theta^C_{i3}c_i^2\right) B_0(m^2_{\tilde\chi^-_a}, m^2_{\tilde e_{i2}}) \\
&\quad - \left(\theta^C_{i3}s^2_\beta + \theta^C_{i4}s_\beta c_\beta\right) B_0(m^2_{\tilde\chi^-_a}, m^2_{H^-}), \\
\mathbf{Q^\tau_{1i}} &= \mathbf{Q^a_{1i}}(m^2_{\tilde\chi^-_a} \to m_\tau), \\
\mathbf{Q^a_{2i}} &= \left(-\theta^C_{i2}c_i s_i + \theta^C_{i4}s_i^2\right) B_0(m^2_{\tilde\chi^-_a}, m^2_{\tilde e_{i1}}) + \left(\theta^C_{i2}s_i c_i + \theta^C_{i4}c_i^2\right) B_0(m^2_{\tilde\chi^-_a}, m^2_{\tilde e_{i2}}) \\
&\quad - \left(\theta^C_{i3}s_\beta c_\beta + \theta^C_{i4}c^2_\beta\right) B_0(m^2_{\tilde\chi^-_a}, m^2_{H^-}), \\
\mathbf{P_{\tilde b\tilde b^c}} &= -c_b s_b B_0(m_b^2, m^2_{\tilde b_1}) + s_b c_b B_0(m_b^2, m^2_{\tilde b_2}) \\
\mathbf{P_{\tilde b^c\tilde b^{c*}}} &= s_b^2 B_0(m_b^2, m^2_{\tilde b_1}) + c_b^2 B_0(m_b^2, m^2_{\tilde b_2}) \\
\mathbf{P_{\tilde b\tilde b^*}} &= c_b^2 B_0(m_b^2, m^2_{\tilde b_1}) + s_b^2 B_0(m_b^2, m^2_{\tilde b_2}), \\
\mathbf{C^a_{ij}} &= \delta_{ij}\left[s_i^2 B_0(m^2_{\tilde\chi^-_a}, m^2_{\tilde e_{i1}}) + c_i^2 B_0(m^2_{\tilde\chi^-_a}, m^2_{\tilde e_{i2}})\right] \\
&\quad + \left(\theta^C_{i3}\theta^C_{j3}s^2_\beta + \theta^C_{i3}\theta^C_{j4}s_\beta c_\beta + \theta^C_{i4}\theta^C_{j3}c_\beta s_\beta + \theta^C_{i4}\theta^C_{j4}c^2_\beta\right) B_0(m^2_{\tilde\chi^-_a}, m^2_{H^-}), \\
\mathbf{J^a} &= s^2_\beta B_0(m^2_{\tilde\chi^-_a}, m^2_{H^-}) \\
&\quad + \theta^C_{i1}\theta^C_{j1}\delta_{ij}\left[c_i^2 B_0(m^2_{\tilde\chi^-_a}, m^2_{\tilde e_{i1}}) + s_i^2 B_0(m^2_{\tilde\chi^-_a}, m^2_{\tilde e_{i2}})\right] \\
&\quad - \theta^C_{i1}\theta^C_{j3}\delta_{ij}c_i s_i\left[B_0(m^2_{\tilde\chi^-_a}, m^2_{\tilde e_{i1}}) - B_0(m^2_{\tilde\chi^-_a}, m^2_{\tilde e_{i2}})\right], \\
\mathbf{B0^a_i} &= c_i^2 B_0(m^2_{\tilde\chi^-_a}, m^2_{\tilde e_{i1}}) + s_i^2 B_0(m^2_{\tilde\chi^-_a}, m^2_{\tilde e_{i2}}) \\
\mathbf{B0^\tau_i} &= \mathbf{B0^a_i}(m^2_{\tilde\chi^-_a} \to m_\tau), \\
\mathbf{H0^a_i} &= -c_i s_i\left[B_0(m^2_{\tilde\chi^-_a}, m^2_{\tilde e_{i1}}) - B_0(m^2_{\tilde\chi^-_a}, m^2_{\tilde e_{i1}})\right], \\
\mathbf{H0^\tau_i} &= \mathbf{H0^a_i}(m^2_{\tilde\chi^-_a} \to m_\tau), \\
\mathbf{E0^a_i} &= \left[c_i^2 B_0(m^2_{\tilde\chi^-_a}, m^2_{\tilde e_{i1}}) + s_i^2 B_0(m^2_{\tilde\chi^-_a}, m^2_{\tilde e_{i2}})\right], \\
\mathbf{E0^\tau_i} &= \mathbf{E0^a_i}(m^2_{\tilde\chi^-_a} \to m_\tau),
\end{aligned}
\tag{A.18}
$$

where

$$
\begin{aligned}
\theta_{ih} &= -s_\alpha(\theta^S_{i1} + \theta^S_{i3}) + c_\alpha(\theta^S_{i2} + \theta^S_{i4}) \\
&= +\xi_i s_\alpha + \eta_i s_\beta m_A^2 \frac{m^2_{\tilde\nu_i}c_{\alpha-\beta} - M_Z^2 c_{2\beta}c_{\alpha+\beta}}{(m^2_{\tilde\nu_i} - m_h^2)(m^2_{\tilde\nu_i} - m_H^2)}, \\
\theta_{iH} &= c_\alpha(\theta^S_{i1} + \theta^S_{i3}) + s_\alpha(\theta^S_{i2} + \theta^S_{i4}) \\
&= -\xi_i c_\alpha + \eta_i s_\beta m_A^2 \frac{m^2_{\tilde\nu_i}s_{\alpha-\beta} - M_Z^2 c_{2\beta}s_{\alpha+\beta}}{(m^2_{\tilde\nu_i} - m_h^2)(m^2_{\tilde\nu_i} - m_H^2)}, \\
\theta_{iA} &= s_\beta(\theta^S_{i1} - \theta^S_{i3}) + c_\beta(-\theta^S_{i2} + \theta^S_{i4}) \\
&= -i\xi_i s_\beta + i\eta_i s_\beta \frac{m_A^2}{m_A^2 - m^2_{\tilde\nu_i}},
\end{aligned}
$$

$$Z_{ij} \;=\; \eta_i\eta_j m_A^4 M_Z^2 c_\beta^2 s_\beta^4 \left[\frac{m^2_{\tilde\nu_i}}{F_S^i} + \frac{m^2_{\tilde\nu_j}}{F_S^j}\right]. \tag{A.19}$$

Here the angle α is the usual diagonalization angle of two CP even Higgs bosons, and $F_S^i \equiv (m^2_{\tilde\nu_i} - m_A^2)(m^2_{\tilde\nu_i} - m_h^2)(m^2_{\tilde\nu_i} - m_H^2)$. Recall that the angle α is defined by $c_{2\alpha} = c_{2\beta}(m_A^2 - M_Z^2)/(m_h^2 - m_H^2)$ and $s_{2\alpha} = s_{2\beta}(m_A^2 + M_Z^2)/(m_h^2 - m_H^2)$. $c_i = \cos\theta_i, s_i = \sin\theta_i$ are the components of the diagonalization matrices of the slepton mass square matrices. $i = \tilde e, \tilde\mu, \tilde\tau$, each. c_b, s_b are the same ones for sbottom mass square matrices. B_0 is the loop function defined as $B_0(x,y) = -\frac{x}{x-y}\ln\frac{x}{y} - \ln\frac{x}{Q^2} + 1$.

APPENDIX B

We collect here 1-loop contributions to the sneutrino minimization condition by calculating all the field-dependent particle masses. As given in the paragraph, the sneutrino vacuum expectation values are given,

$$\xi_i \equiv \frac{\langle\tilde\nu_i\rangle}{\langle H_1^0\rangle} = -\frac{m^2_{L_iH_1} + B_i t_\beta + \Sigma^{(1)}_{L_i}}{m^2_{\tilde\nu_i} + \Sigma^{(2)}_{L_i}}, \tag{B.1}$$

where the 1-loop contributions $\Sigma^{(1,2)}_{L_i}$ are given by $\Sigma^{(1)}_{L_i} = \partial V_1/H_1^*\partial L_i$, $\Sigma^{(2)}_{L_i} = \partial V_1/L_i^*\partial L_i$. Here, we will give the explicit forms of these Σ_{L_i}'s.

1. Top squark contribution

The contributions from the stop mass eigenstates $\tilde t_{1,2}$ as follows:

$$\Sigma^{(1)}_{L_i}(\tilde t_j) = \frac{6}{64\pi^2}\left\{\frac{4M^2_{Dt}}{2m^2_{\tilde t_j} - m^2_{\tilde t_1} - m^2_{\tilde t_2}}\frac{m_t\mu_i}{v^2 s_{2\beta}/2}\right\} m^2_{\tilde t_j}\left(\ln\frac{m^2_{\tilde t_j}}{Q^2} - 1\right), \tag{B.2}$$

$$\Sigma^{(2)}_{L_i}(\tilde t_j) = \frac{6}{64\pi^2}\left\{\frac{1}{2}\frac{M_Z^2}{v^2} + \frac{M^2_{Lt} - M^2_{Rt}}{2m^2_{\tilde t_j} - m^2_{\tilde t_1} - m^2_{\tilde t_2}}\frac{8M_W^2 - 5M_Z^2}{6v^2}\right\} m^2_{\tilde t_j}\left(\ln\frac{m^2_{\tilde t_j}}{Q^2} - 1\right), \tag{B.3}$$

where $M^2_{Lt} = \mathcal{M}^2_{\tilde t,11}$, $M^2_{Dt} = \mathcal{M}^2_{\tilde t,12}$ and $M^2_{Rt} = \mathcal{M}^2_{\tilde t,22}$ ignoring small R-parity violating contributions.

2. Bottom squark contribution

The sbottom contributions are

$$\Sigma^{(1)}_{L_i}(\tilde b_j) = \frac{6}{64\pi^2}\left\{2\lambda'_i\frac{m_b}{v_1} + \frac{4M^2_{Db}}{2m^2_{\tilde b_j} - m^2_{\tilde b_1} - m^2_{\tilde b_2}}\frac{A'_i}{v_1}\right\} m^2_{\tilde b_j}\left(\ln\frac{m^2_{\tilde b_j}}{Q^2} - 1\right), \tag{B.4}$$

$$\Sigma^{(2)}_{L_i}(\tilde b_j) = \frac{6}{64\pi^2}\left\{-\frac{1}{2}\frac{M_Z^2}{v^2} + \frac{M^2_{Lb} - M^2_{Rb}}{2m^2_{\tilde b_j} - m^2_{\tilde b_1} - m^2_{\tilde b_2}}\frac{-4M_W^2 + M_Z^2}{6v^2}\right\} m^2_{\tilde t_j}\left(\ln\frac{m^2_{\tilde t_j}}{Q^2} - 1\right), \tag{B.5}$$

where M^2_{Lb}, M^2_{Rb}, and M^2_{Db} are defined as in the stop case. The contributions from the first two squark generations can be obtained by obvious substitutions.

3. Charged slepton or charged Higgs contributions

Let us denote the charged slepton and Higgs contributions to Σ's as

$$\Sigma^{(1,2)}_{L_j}(\phi) = \frac{4}{64\pi^2} S_j^{(1,2)}(\phi) m_\phi^2\left(\ln\frac{m_\phi^2}{Q^2} - 1\right), \tag{B.6}$$

where ϕ stands for the mass eigenstates $\tilde{e}_{i1}, \tilde{e}_{i2}$ and H^-. Here $S_j^{(1)}(\phi) \equiv (\partial m_\phi^2/\partial u_j)/2v_1$ and $S_j^{(2)}(\phi) \equiv (\partial m_\phi^2/\partial u_j)/2u_j$. $M_{L_i}^2 = \mathcal{M}_{i,11}^2, M_{D_i}^2 = \mathcal{M}_{i,12}^2$ and $M_{R_i}^2 = \mathcal{M}_{i,22}^2$. Where i runs $\tilde{e}, \tilde{\mu}, \tilde{\tau}$. ignoring small R-parity violating contributions.

4. Charged Higgs contributions

For $i = 1, 2$,

$$S_j^{(1)}(H^-) = \frac{s_{2\beta} M_W^2 (B_i - m_{L_i H_1}^2 t_\beta)}{v^2 (M_{L_i}^2 - m_{H^-}^2)}. \tag{B.7}$$

For $i = 3$,

$$S_3^{(1)}(H^-) = \frac{(c_\beta B_3 - s_\beta m_{L_3 H_1}^2)((m_{H^-}^2 - M_{R_3}^2)(m_\tau^2 - 2M_W^2)s_\beta + \mu m_\tau M_{D_3}^2)}{v^2 (m_{H^-}^2 - m_{\tilde{\tau}_1}^2)(m_{H^-}^2 - m_{\tilde{\tau}_2}^2)}. \tag{B.8}$$

For $i = 1, 2$,

$$S_i^{(2)}(H^-) = \frac{(m_{H^-}^2 - M_{L_i}^2)(2M_W^2 - M_Z^2)c_{2\beta} + 2M_W^4 s_{2\beta}^2}{2v^2 (m_{H^-}^2 - M_{L_i}^2)}. \tag{B.9}$$

For $i = 3$,

$$\begin{aligned} S_3^{(2)}(H^-) & \\ = \{ \quad & ((m_{H^-}^2 - m_{\tilde{\tau}_1}^2)(m_{H^-}^2 - m_{\tilde{\tau}_2}^2)(2M_W^2 - M_Z^2 - m_\tau^2)c_{2\beta} \\ - \; & 2(m_{H^-}^2 - M_{R_3}^2)s_{2\beta}^2(M_W^4 + M_W^2 m_\tau^2 + m_\tau^4) - 2(m_{H^-}^2 - M_{L_3}^2)c_\beta^2 \mu^2 m_\tau^2 \\ + \; & 4 s_\beta c_\beta^2 \mu m_\tau (-m_\tau^2 + 2M_W^2) M_{D_3}^2 \} \; / \; 2v^2 (m_{H^-}^2 - m_{\tilde{\tau}_1}^2)(m_{H^-}^2 - m_{\tilde{\tau}_2}^2). \end{aligned} \tag{B.10}$$

5. Scalar Lepton contributions

$$S_1^{(1)}(\tilde{e}_L) = \frac{M_W^2 (t_\beta (m_{H^-}^2 c_{2\beta} + M_{L_1}^2) B_1 + (m_{H^-}^2 c_{2\beta} - M_{L_1}^2) m_{L_1 H_1}^2)}{v^2 M_{L_1}^2 (m_{H^-}^2 - M_{L_1}^2)}. \tag{B.11}$$

$$S_{2,3}^{(1)}(\tilde{e}_L) = 0. \tag{B.12}$$

$$S_i^{(1)}(\tilde{e}_R) = 0, \qquad i = 1, 3 \tag{B.13}$$

$$S_2^{(1)}(\tilde{\mu}_L) = \frac{M_W^2 (t_\beta (m_{H^-}^2 c_{2\beta} + M_{L_2}^2) B_2 + (m_{H^-}^2 c_{2\beta} - M_{L_2}^2) m_{L_2 H_1}^2)}{v^2 M_{L_2}^2 (m_{H^-}^2 - M_{L_2}^2)}. \tag{B.14}$$

$$S_{1,3}^{(1)}(\tilde{\mu}_L) = 0. \tag{B.15}$$

$$S_i^{(1)}(\tilde{\mu}_R) = 0, \qquad i = 1, 3 \tag{B.16}$$

$$S_1^{(2)}(\tilde{e}_L) = \frac{(m_{H^-}^2 - M_{L_1}^2)(M_Z^2 M_{L_1}^2 + 2M_W^4) - 2M_W^4 m_{H^-}^2 s_{2\beta}^2}{2v^2 M_{L_1}^2 (m_{H^-}^2 - M_{L_1}^2)}. \tag{B.17}$$

$$S^{(2)}_{2,3}(\tilde{e}_L) = \frac{-2M_W^2 + M_Z^2}{2v^2}. \tag{B.18}$$

$$S^{(2)}_{i}(\tilde{e}_R) = \frac{M_W^2 - M_Z^2}{v^2}, \qquad i = 1,3 \tag{B.19}$$

$$S^{(2)}_{2}(\tilde{\mu}_L) = \frac{(m_{H^-}^2 - M_{L_2}^2)(M_Z^2 M_{L_2}^2 + 2M_W^4) - 2M_W^4 m_{H^-}^2 s_{2\beta}^2}{2v^2 M_{L_2}^2 (m_{H^-}^2 - M_{L_2}^2)}. \tag{B.20}$$

$$S^{(2)}_{1,3}(\tilde{\mu}_L) = \frac{-2M_W^2 + M_Z^2}{2v^2}. \tag{B.21}$$

$$S^{(2)}_{i}(\tilde{\mu}_R) = \frac{M_W^2 - M_Z^2}{v^2}, \qquad i = 1,3 \tag{B.22}$$

For $i = 1,2$

$$S^{(1)}_{i}(\tilde{\tau}_{1,2}) = -\frac{m_\tau}{v}\lambda_i \mp \frac{M_{D_3}^2 t_\beta}{m_{\tilde{\tau}_2}^2 - m_{\tilde{\tau}_1}^2}\lambda_i. \tag{B.23}$$

For $i = 3$,

$$S^{(1)}_{3}(\tilde{\tau}_{1,2}) = -\frac{(A)\cdot B_3 + (B)\cdot m_{L_3H_1}^2 \mp \frac{(C)\cdot B_3 + (D)\cdot m_{L_3H_1}^2}{m_{\tilde{\tau}_2}^2 - m_{\tilde{\tau}_1}^2}}{2v^2 c_\beta m_{\tilde{\tau}_2}^2 m_{\tilde{\tau}_1}^2 (m_{H^-}^2 - m_{\tilde{\tau}_1}^2)(m_{H^-}^2 - m_{\tilde{\tau}_2}^2)}, \tag{B.24}$$

where,

$$\begin{aligned}
(A) = &\quad (m_{H^-}^2 - m_{\tilde{\tau}_1}^2)(m_{H^-}^2 - m_{\tilde{\tau}_2}^2)(M_{D_3}^2 \mu m_\tau + M_{R_3}^2 s_\beta M_W^2) \\
&+ m_{H^-}^2 (M_{R_3}^2 (M_{R_3}^2 - m_{H^-}^2) + M_{D_3}^4)(2M_W^2 - c_\beta m_\tau^2) s_\beta c_\beta \\
&+ M_{D_3}^2 m_{H^-}^2 (m_{\tilde{\tau}_2}^2 + m_{\tilde{\tau}_1}^2 - m_{H^-}^2)\mu m_\tau c_\beta^2, \\
(B) = &\quad (M_{R_3}^2 m_{H^-}^4 - M_{R_3}^4 M_{L_3}^2 + M_{R_3}^2 M_{D_3}^4 \\
&\quad - M_{R_3}^4 m_{H^-}^2 + M_{L_3}^2 M_{R_3}^2 m_{H^-}^2 - 2M_{D_3}^4 m_{H^-}^2) c_\beta M_W^2 \\
&- m_{\tilde{\tau}_2}^2 m_{\tilde{\tau}_1}^2 (m_{H^-}^2 - M_{R_3}^2) c_\beta m_\tau^2 + M_{D_3}^2 m_{H^-}^2 (m_{H^-}^2 - m_{\tilde{\tau}_2}^2 - m_{\tilde{\tau}_1}^2) s_\beta c_\beta \mu m_\tau \\
&+ m_{H^-}^2 (M_{R_3}^2 (M_{R_3}^2 - m_{H^-}^2) + M_{D_3}^4)(2M_W^2 - m_\tau^2) c_\beta^3, \\
(C) = &- (m_{H^-}^2 - m_{\tilde{\tau}_1}^2)(m_{H^-}^2 - m_{\tilde{\tau}_2}^2) \\
&\qquad \times (M_{D_3}^2 (m_{\tilde{\tau}_1}^2 + m_{\tilde{\tau}_2}^2)\mu m_\tau + (2M_{D_3}^4 + M_{R_3}^2 (M_{R_3}^2 - M_{L_3}^2)) s_\beta M_W^2) \\
&- M_{D_3}^2 m_{H^-}^2 ((m_{\tilde{\tau}_1}^2 + m_{\tilde{\tau}_2}^2)(m_{\tilde{\tau}_1}^2 + m_{\tilde{\tau}_2}^2 - m_{H^-}^2) - 2m_{\tilde{\tau}_1}^2 m_{\tilde{\tau}_2}^2) c_\beta^2 \mu m_\tau \\
&+ m_{H^-}^2 (M_{R_3}^6 - (M_{L_3}^2 + m_{H^-}^2) M_{R_3}^4 + (m_{H^-}^2 M_{L_3}^2 + 3M_{D_3}^4) M_{R_3}^2 \\
&\quad + (M_{L_3}^2 - 2m_{H^-}^2) M_{D_3}^4)(m_\tau^2 - 2M_W^2) s_\beta c_\beta^2, \\
(D) = &- m_{\tilde{\tau}_1}^2 m_{\tilde{\tau}_2}^2 ((M_{R_3}^2 - M_{L_3}^2)(M_{R_3}^2 - m_{H^-}^2) + 2M_{D_3}^4) c_\beta m_\tau^2 \\
&+ (-2M_{D_3}^8 + (-M_{R_3}^4 + 4M_{R_3}^2 m_{H^-}^2 - 2m_{H^-}^4 + 3M_{L_3}^2 M_{R_3}^2) M_{D_3}^4 \\
&\qquad + M_{R_3}^2 (M_{L_3}^2 + m_{H^-}^2)(M_{R_3}^2 - m_{H^-}^2)(M_{R_3}^2 - M_{L_3}^2)) c_\beta M_W^2 \\
&+ M_{D_3}^2 m_{H^-}^2 ((m_{\tilde{\tau}_1}^2 + m_{\tilde{\tau}_2}^2)(m_{\tilde{\tau}_1}^2 + m_{\tilde{\tau}_2}^2 - m_{H^-}^2) - 2m_{\tilde{\tau}_1}^2 m_{\tilde{\tau}_2}^2) s_\beta c_\beta \mu m_\tau \\
&+ (M_{R_3}^6 - (M_{L_3}^2 + m_{H^-}^2) M_{R_3}^4 + (m_{H^-}^2 M_{L_3}^2 + 3M_{D_3}^4) M_{R_3}^2 \\
&\qquad + (M_{L_3}^2 - 2m_{H^-}^2) M_{D_3}^4)(m_\tau^2 - M_W^2) c_\beta^3.
\end{aligned} \tag{B.25}$$

For $i = 1,2$,

$$S^{(2)}_{i}(\tilde{\tau}_{1,2}) = -\frac{M_Z^2}{4v^2}\Big(1 \mp \frac{(M_{L_3}^2 - M_{R_3}^2)(4M_W^2 - 3M_Z^2)}{M_Z^2 (m_{\tilde{\tau}_2}^2 - m_{\tilde{\tau}_1}^2)}\Big). \tag{B.26}$$

For $i = 3$,

$$S_3^{(2)}(\tilde{\tau}_{1,2}) = -\frac{(E) \mp \frac{(F)}{m_{\tilde{\tau}_2}^2 - m_{\tilde{\tau}_1}^2}}{4v^2 m_{\tilde{\tau}_2}^2 m_{\tilde{\tau}_1}^2 (m_{H^-}^2 - m_{\tilde{\tau}_1}^2)(m_{H^-}^2 - m_{\tilde{\tau}_2}^2)}, \tag{B.27}$$

where,

$$\begin{aligned}
(E) = & - (m_{H^-}^2 - m_{\tilde{\tau}_1}^2)(m_{H^-}^2 - m_{\tilde{\tau}_2}^2) \\
& \times (m_{\tilde{\tau}_1}^2 m_{\tilde{\tau}_2}^2 (2M_W^2 - M_Z^2) + 2M_{L_3}^2 \mu^2 m_\tau^2 + 4M_{D_3}^2 \mu M_W^2 m_\tau s_\beta - 2M_{R_3}^2 M_W^4) \\
& + 4M_{D_3}^2 m_{H^-}^2 (m_{\tilde{\tau}_1}^2 + m_{\tilde{\tau}_2}^2 - m_{H^-}^2)(\mu m_\tau^3 - 2\mu m_\tau M_W^2) s_\beta c_\beta^2 \\
& - 8m_{H^-}^2 (M_{D_3}^4 + M_{R_3}^4 - M_{R_3}^2 m_{H^-}^2)(c_\beta^2 s_\beta^2 M_W^4 - c_\beta^4 m_\tau^4 + c_\beta^4 M_W^2 m_\tau^2) \\
& - 2m_{H^-}^2 (M_{D_3}^4 + M_{L_3}^4 - M_{L_3}^2 m_{H^-}^2) c_\beta^2 \mu^2 m_\tau^2 \\
& + 4((2m_{H^-}^2 - M_{R_3}^2) M_{D_3}^4 + M_{R_3}^2 (M_{L_3}^2 + m_{H^-}^2)(M_{R_3}^2 - m_{H^-}^2)) c_\beta^2 M_W^2 m_\tau^2 \\
& - 2m_{\tilde{\tau}_1}^2 m_{\tilde{\tau}_2}^2 (M_{R_3}^2 - m_{H^-}^2) c_\beta^2 m_\tau^4, \\
(F) = & \quad (m_{H^-}^2 - m_{\tilde{\tau}_1}^2)(m_{H^-}^2 - m_{\tilde{\tau}_2}^2) \\
& \quad \times \Big[m_{\tilde{\tau}_1}^2 m_{\tilde{\tau}_2}^2 (M_{L_3}^2 - M_{R_3}^2)(3M_Z^2 - 2M_W^2) \\
& \qquad -2(m_{\tilde{\tau}_1}^2 m_{\tilde{\tau}_2}^2 - M_{D_3}^4 - M_{L_3}^4) \mu^2 m_\tau^2 \\
& \qquad +4M_{D_3}^2 (M_{L_3}^2 + M_{R_3}^2) s_\beta \mu M_W^2 m_\tau \\
& \qquad -2(m_{\tilde{\tau}_1}^2 m_{\tilde{\tau}_2}^2 - M_{D_3}^4 - M_{R_3}^4) M_W^4 \Big] \\
& + 2((m_{\tilde{\tau}_1}^2 + m_{\tilde{\tau}_2}^2)(m_{\tilde{\tau}_1}^2 + m_{\tilde{\tau}_2}^2 - m_{H^-}^2) - 2m_{\tilde{\tau}_1}^2 m_{\tilde{\tau}_2}^2) \\
& \quad \times \Big[(M_{L_3}^2 M_{R_3}^2 - m_{H^-}^4) c_\beta^2 m_\tau^4 - 2M_{D_3}^2 m_{H^-}^2 s_\beta c_\beta^2 \mu (m_\tau^3 - 2M_W^2 m_\tau) \Big] \\
& + 2m_{H^-}^2 (s_{2\beta}^2 M_W^4 + c_\beta^4 (4M_W^2 m_\tau^2 - m_\tau^4)) \\
\times & \Big[M_{R_3}^6 - (M_{L_3}^2 + m_{H^-}^2) M_{R_3}^4 + (m_{H^-}^2 M_{L_3}^2 + 3M_{D_3}^4) M_{R_3}^2 + M_{D_4}^4 (M_{L_3}^2 - 2m_{H^-}^2) \Big] \\
& + 2m_{H^-}^2 c_\beta^2 \mu^2 m_\tau^2 \\
\times & \Big[M_{L_3}^6 - (M_{R_3}^2 + m_{H^-}^2) M_{L_3}^4 + (m_{H^-}^2 M_{R_3}^2 + 3M_{D_3}^4) M_{L_3}^2 + M_{D_4}^4 (M_{R_3}^2 - 2m_{H^-}^2) \Big] \\
& + \Big[8M_{D_3}^8 + 4(M_{R_3}^4 - (3M_{L_3}^2 + 4m_{H^-}^2) M_{R_3}^2 + 2m_{H^-}^4) M_{D_3}^4 \\
& \qquad -4M_{R_3}^2 (M_{L_3}^2 + m_{H^-}^2)(M_{R_3}^2 - M_{L_3}^2)(M_{R_3}^2 - m_{H^-}^2) \Big] c_\beta^2 M_W^2 m_\tau^2.
\end{aligned} \tag{B.28}$$

6. Neutrino-Neutralino contributions

The sneutrino VEVs contributions are

$$\Sigma_{L_i}^{(1,2)}(\psi) = -\frac{8}{64\pi^2} S_i^{(1,2)}(\psi) m_\psi^2 \left(\ln \frac{m_\psi^2}{Q^2} - 1 \right), \tag{B.29}$$

where ψ runs for four neutralinos $\tilde{\chi}_i^0$. For 4 neutralinos, $\Psi = \tilde{\chi}_i^0, i = 1, 4$,

$$\begin{aligned}
S_i^{(2)}(\Psi) = \frac{2\mu M_Z^2}{v^2} m_\Psi \Big[& - \mu M_{\tilde{\gamma}} m_\Psi^3 + (-s_{2\beta} M_Z^2 M_{\tilde{\gamma}} + \mu (M_1^2 c_W^2 + M_2^2 s_W^2)) m_\Psi^2 \\
& + M_{\tilde{\gamma}} (s_{2\beta} M_Z^2 M_{\tilde{\gamma}} + \mu (M_Z^2 + \mu)) m_\Psi \\
& - (M_Z^2 M_{\tilde{\gamma}}^2 + \mu^2 (M_1^2 c_W^2 + M_2^2 s_W^2)) \Big] \ / \ D(\Psi),
\end{aligned} \tag{B.30}$$

where,

$$D(\Psi) = \det(M_N)\Big[\quad 4m_\Psi^3 - 3(M_1+M_2)m_\Psi^2 + 2(M_1M_2 - M_Z^2 - \mu^2)m_\Psi + M_Z^2(M_{\tilde\gamma} + s_{2\beta}\mu) + \mu^2(M_1+M_2) \Big], \tag{B.31}$$

$$M_{\tilde\gamma} = M_1 c_W^2 + M_2 s_W^2, \tag{B.32}$$

$$\det M_N = -\mu(\mu M_1 M_2 + s_{2\beta}(M_1 M_W^2 + M_2(M_Z^2 - M_W^2))). \tag{B.33}$$

7. CP-even sneutrino or Higgs boson contributions

As in the above case, we write

$$\Sigma_{L_i}^{(1,2)}(\phi) = \frac{2}{64\pi^2} S_i^{(1,2)}(\phi) m_\phi^2 \left(\ln\frac{m_\phi^2}{Q^2} - 1\right), \tag{B.34}$$

where ϕ runs for $\mathrm{Re}(\tilde\nu)$, h^0 and H^0 and $S_i^{(1),(2)}(\phi)$ are calculated as follows:

$$S_j^{(1)}(\tilde\nu_i) = -\frac{\delta_{ij}}{F_i}\frac{M_Z^2}{v^2}\Big[(m_A^2 c_{2\beta} - M_{\tilde\nu_i}^2)m_{L_iH_1}^2 + t_\beta(m_A^2 c_{2\beta} + M_{\tilde\nu_i}^2)B_i\Big], \tag{B.35}$$

$$S_j^{(2)}(\tilde\nu_i) = \frac{M_Z^2}{2v^2}\Big[1 + \delta_{ij}\Big(\frac{3M_{\tilde\nu_i}^4 + (3m_A^2 + M_Z^2)M_{\tilde\nu_i}^2 - m_{H^0}^2 m_{h^0}^2}{F_i} - 1\Big)\Big], \tag{B.36}$$

$$\begin{aligned} S_i^{(1)}(h^0,H^0) = \frac{M_Z^2}{v^2}\frac{1}{F_i}\Big[\quad & ((m_A^2 c_{2\beta} - M_{\tilde\nu_i}^2)m_{L_iH_1}^2 + t_\beta(m_A^2 c_{2\beta} + M_{\tilde\nu_i}^2)B_i) \\ \mp \; & \frac{1}{m_{H^0}^2 - m_{h^0}^2}\{t_\beta(-(m_{H^0}^2 + m_{h^0}^2 + 2m_A^2 c_{2\beta})M_{\tilde\nu_i}^2 \\ & \quad + m_A^2(m_A^2 c_{2\beta} + M_Z^2 c_{2\beta}(4c_\beta^2 - 1)))B_i \\ & \quad + ((m_{H^0}^2 + m_{h^0}^2 - 2m_A^2 c_{2\beta})M_{\tilde\nu_i}^2 \\ & \quad + m_A^2 c_{2\beta}(m_A^2 - M_Z^2(4c_\beta^2 - 3)))m_{L_iH_1}^2\}\Big], \end{aligned} \tag{B.37}$$

$$\begin{aligned} S_i^{(2)}(h^0,H^0) = -\frac{M_Z^2}{2v^2F_i}\Big[\quad & M_Z^2(M_{\tilde\nu_i}^2 - M_A^2 c_{2\beta}^2) \\ \mp \; & \frac{1}{m_{H^0}^2 - m_{h^0}^2}\{\, c_{2\beta}(m_A^2 - M_Z^2)M_{\tilde\nu_i}^4 \\ & \quad + (-m_A^4 c_{2\beta} + M_Z^2 m_A^2(2s_{2\beta}^2 - 1) + 2M_Z^4 c_\beta^2)M_{\tilde\nu_i}^2 \\ & \quad + 2M_Z^2 m_A^2 c_\beta c_{2\beta}(m_A^2 - M_Z^2)\,\}\Big], \end{aligned} \tag{B.38}$$

where,

$$F_i = M_{\tilde\nu_i}^4 - (m_{H^0}^2 + m_{h^-}^2)M_{\tilde\nu_I}^2 + m_{H^0}^2 m_{h^0}^2. \tag{B.39}$$

Also note that $M_{\tilde\nu_i}^2$'s are the usual R-parity conserving sneutrino masses.

8. CP-odd sneutrino or Higgs boson contributions

$$\Sigma^{(1,2)}_{L_j}(\phi) = \frac{2}{64\pi^2} S^{(1,2)}_i(\phi) m^2_\phi \left(\ln \frac{m^2_\phi}{Q^2} - 1 \right), \tag{B.40}$$

where ϕ runs for $\mathrm{Im}(\tilde{\nu})$, A^0. Here, $S^{(1),(2)}_i(\phi)$ are given by

$$S^{(1)}_j(\tilde{\nu}^I_i) = 0, \tag{B.41}$$

$$S^{(2)}_j(\tilde{\nu}^I_i) = \frac{1}{2}\frac{M^2_Z}{v^2}, \tag{B.42}$$

$$S^{(1)}_i(A^0) = 0, \tag{B.43}$$

$$S^{(2)}_i(A^0) = -\frac{1}{2}\frac{M^2_Z}{v^2}\cos 2\beta. \tag{B.44}$$

9. Charged lepton or chargino contribution

Neglecting the contributions from the two light charged leptons by taking $m_{e,\mu} = 0$, we get

$$\Sigma^{(1,2)}_{L_i}(\Psi) = -\frac{8}{64\pi^2} S^{(1,2)}_i(\Psi) m^2_\Psi \left(\ln \frac{m^2_\Psi}{Q^2} - 1 \right), \tag{B.45}$$

where Ψ runs for τ and the charginos $\tilde{\chi}^-_{1,2}$ and $S^{(1,2)}(\Psi)$ are given by

$$S^{(1)}_i(\Psi) = -\lambda_i m_\tau \frac{m^2_\Psi}{v_1} \left[(m^2_\Psi - m^2_{\tilde{\chi}^+_1})(m^2_\Psi - m^2_{\tilde{\chi}^+_2}) \right] / D(\Psi), \tag{B.46}$$

$$\begin{aligned} S^{(2)}_i(\Psi) = 2\frac{m^2_\Psi}{v} \Big[& \quad m^4_\Psi M^2_W - m^2_\Psi M^2_W(\mu^2 + 2M^2_W s^2_\beta \\ & + \; m^2_\tau) + m^2_\tau M^2_W(\mu^2 + 2M^2_W s^2_\beta) \\ & + \; \delta_{ij} m^2_\tau \{ \; m^4_\Psi/2c^2_\beta + m^2_\Psi[M^2_W(3 - t^2_\beta) - M^2_2/c^2_\beta] \\ & \qquad\qquad - 2M^2_W(M_2\mu t_\beta - 3M^2_W s^2_\beta - \mu^2)\} \; \Big] / D(\Psi), \end{aligned} \tag{B.47}$$

where,

$$\begin{aligned} D(\Psi) = & \quad 5m^6_\Psi - 4m^4_\Psi(m^2_{\tilde{\chi}^-_1} + m^2_{\tilde{\chi}^-_2} + m^2_\tau) \\ & + \; 3m^2_\Psi[m^2_\tau(m^2_{\tilde{\chi}^-_1} + m^2_{\tilde{\chi}^-_2}) + m^2_{\tilde{\chi}^-_1} m^2_{\tilde{\chi}^-_2}] - 2m^2_\tau m^2_{\tilde{\chi}^-_1} m^2_{\tilde{\chi}^-_2}. \end{aligned} \tag{B.48}$$

[1] Y. Fukuda *et al.* [Super-Kamiokande Collaboration], Phys. Rev. Lett. **81** 1562 (1998) ; M. Apollonio *et al.* [CHOOZ Collaboration], Phys. Lett. **B420** 397 (1998); Q. R. Ahmad *et al.* [SNO Collaboration], Phys. Rev. Lett. **87** 071301 (2001); S. Fukuda *et al.* [Super-Kamiokande Collaboration], Phys. Lett. **B539** 179 (2002) ; K. Eguchi *et al.* [KamLAND Collaboration], Phys. Rev. Lett. **90** 021802 (2003); M. H. Ahn *et al.* [K2K Collaboration], Phys. Rev. Lett. **90** 041801 (2003) **90** 041801 (2003).

[2] L. Hall and Suzuki, Nucl. Phys. **B231** 419 (1984); A. S. Joshipura and M. Nowakowski, Phys. Rev. **D51** 2421 (1995) ; M. Nowakowski and A. Pilaftsis, Nucl. Phys. **B461** 19 (1996) ; F. M. Borzumati, Y. Grossman, E. Nardi and Y. Nir, Phys. Lett. **B384** 123 (1996); B. de Carlos and P.L. White, Phys. Rev. **D54** 3427 (1996); A. Yu. Smirnov and F. Vissani, Nucl. Phys. **B460** 37 (1996); R. Hempfling, Nucl. Phys. **B478** 3 (1996) ; H.P. Nilles and N. Polonsky, Nucl. Phys. **B484** 33 (1997) ; E. Nardi, Phys. Rev. **D55** 5772 (1997); M. Drees, *et al.*, Phys. Rev. **D57** 5335 (1998); E. J. Chun, *et al.*, Nucl. Phys. **B544** 89 (1999); A. S. Joshipura and S.K. Vempati, Phys. Rev. **D60** r (095009)1999; Phys. Rev. **D60** 111303 (1999); K. Choi, *et al.*, Phys. Rev. **D60** 031301 (1999); O. Kong, Mod. Phys. Lett. **A14** 903 (1999); S. Rakshit, *et al.*, Phys. Rev. **D59** 091701 (1999); R. Adhikari, G. Omanovic, Phys. Rev. **D59** 073003 (1999); Y. Grossman and H. E. Haber, Phys. Rev. **D59** 093008 (1999); D. E. Kaplan and A. Nelson, JHEP **0001** 033 (2000); J. L. Chkareuli, *et al.*, Phys. Rev. **D 62** 015014 (2000); O. Haug, *et al.*, Nucl. Phys. **B 565** 38 (2000); S. Davidson and M. Losada, JHEP **0005** 021 (2000); F. Takayama and M. Yamaguchi, Phys. Lett. **B476** 116 (2000); S. K. Kang and O. W. Kong, hep-ph/0206009.

[3] H. Dreiner and G.G. Ross, Nucl. Phys. **B365** 597 (1991); D. P. Roy, Phys. Lett. **B128** 270 (1992); R. M. Godbole, P. Roy and X. Tata, Nucl. Phys. **B401** 67 (1993).

[4] B. Mukhopadhyaya, S. Roy and F. Vissani, Phys. Lett. **B443** 191 (1998); A. Datta, B. Mukhopadhyaya and F. Vissani, Phys. Lett. **B492** 324 (2000).

[5] E.J. Chun and J.S. Lee, Phys. Rev. **D60** 075006 (1999); S.Y. Choi, E.J. Chun, S.K. Kang and J.S. Lee, Phys. Rev. **D60** 075002 (1999).

[6] W. Porod, M. Hirsch J.C. Romao and J.W.F. Valle, Phys. Rev. **D63** 115004 (2001). A. Bartl, M. Hirsch, T. Kernreiter, W. Porod and J.W.F. Valle, hep-ph/0206071.

[7] E.J. Chun, D.W. Jung, S.K. Kang and J.D. Park, Phys. Rev. **D66** 073003 (2002); E.J. Chun, D.W. Jung and S.K. Kang, work in progress.

[8] M.A. Diaz, R.A. Lineros and M.A. Rivera, Phys. Rev. **D67** 115004 (2003).

[9] B.C. Allanach, A. Dedes and H.K. Dreiner, hep-ph/0309196.

[10] E.J. Chun and S.K Kang, Phys. Rev. **D61** 075012 (2000).

[11] M. Hirsch *et. al.*, Phys. Rev. **D62** 113008 (2000) [Erratum-ibid.Phys. Rev. **D65** 119901 (2002)].

[12] A. Abada, S. Davidson and M. Losada, Phys. Rev. **D65** 075010 (2002); A.S. Joshipura, R.D. Vaidya and S.K. Vempati, hep-ph/0203182.

[13] E. J. Chun, D. W. Jung and J. D. Park, Phys. Lett. **B557** 233 (2003)

[14] ECFA/DESY LC Physics working group, J. A. Aguillar-Saavedra et al., hep-ph/0106315.

[15] ECFA/DESY SUSY, A. Bartl et al., hep-ph/0301027.

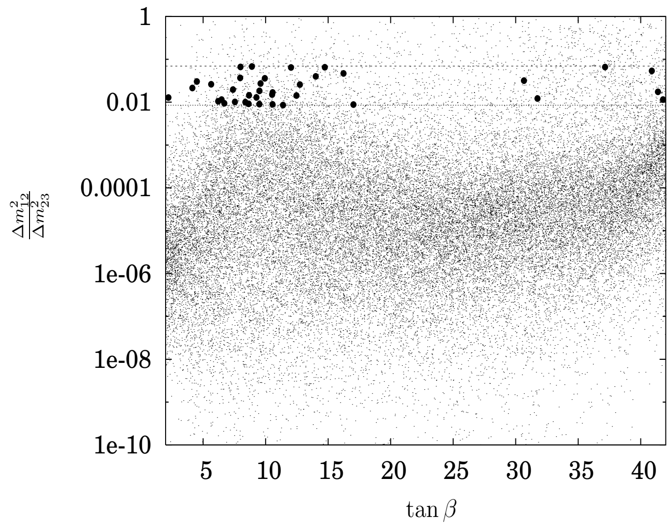

FIG. 1: The ratio $\Delta m_{sol}^2/\Delta m_{atm}^2$ for general points. The region between the two straight lines is allowed by the neutrino data and big dots are the solution points accomodating the observed mixing angles.

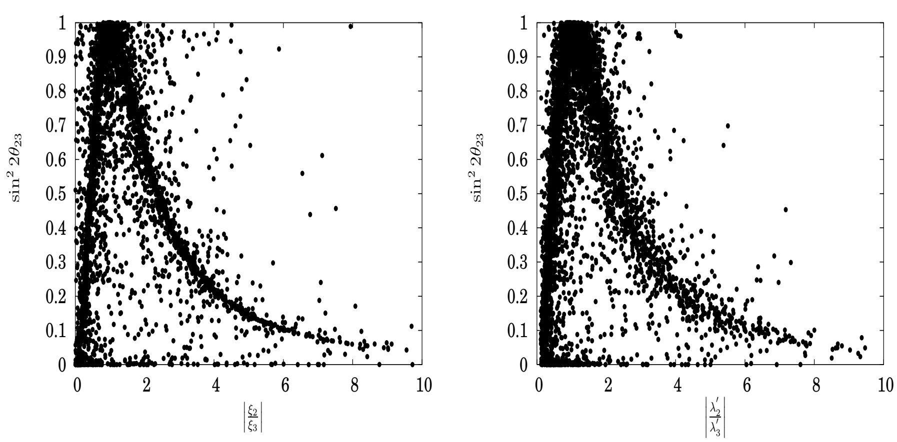

(a) $\sin^2 2\theta_{23}$ vs. $|\xi_2/\xi_3|$

(b) $\sin^2 2\theta_{23}$ vs. $\left|\lambda_2'/\lambda_3'\right|$

FIG. 2: The atmospheric neutrino mixing angle vs. $|\xi_2/\xi_3|$ and $|\lambda_2'/\lambda_3'|$ for general points.

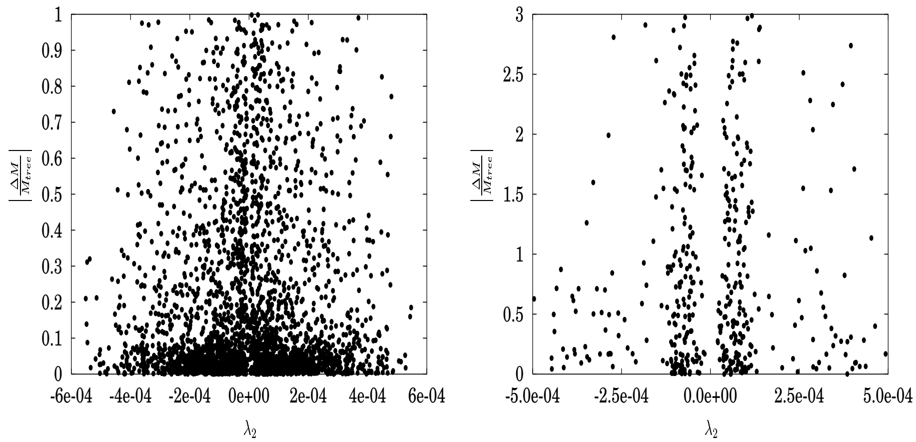

(a) For general points

(b) For solution points

FIG. 3: The ratio $|m_3 - m_3^0|/m_3^0$ for the loop-corrected (m_3) and tree-level (m_3^0) neutrino masses with varying λ_2.

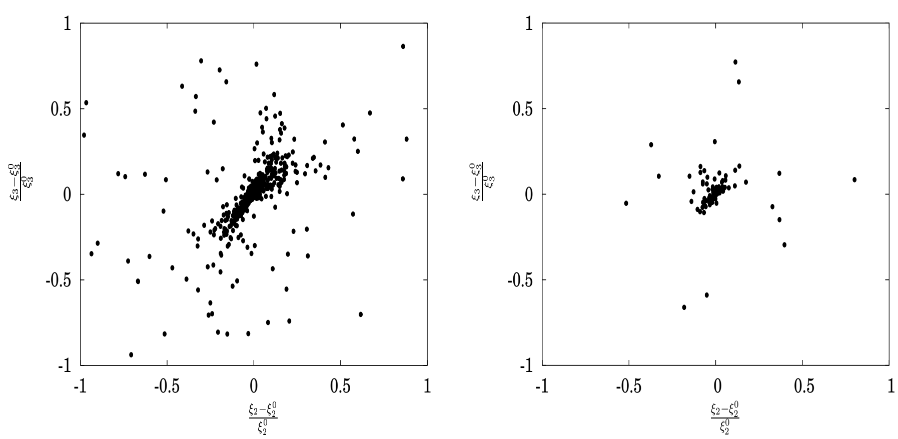

(a) For $\tan\beta = 3 - 15$

(b) For $\tan\beta = 30 - 40$

FIG. 4: Plots for $(\xi_3 - \xi_3^0)/\xi_3^0$ versus $(\xi_2 - \xi_2^0)/\xi_2^0$ showing the effect of SVEV 1-loop correction for solution points

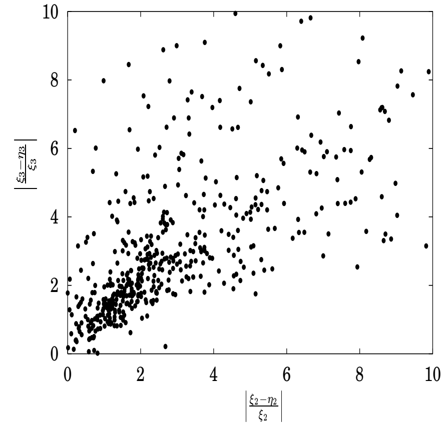

FIG. 5: Plots for $|(\xi_3 - \eta_3)/\xi_3|$ versus $|(\xi_2 - \eta_2)/\xi_2|$ showing the deviation of η_i from ξ_i direction for solution points.

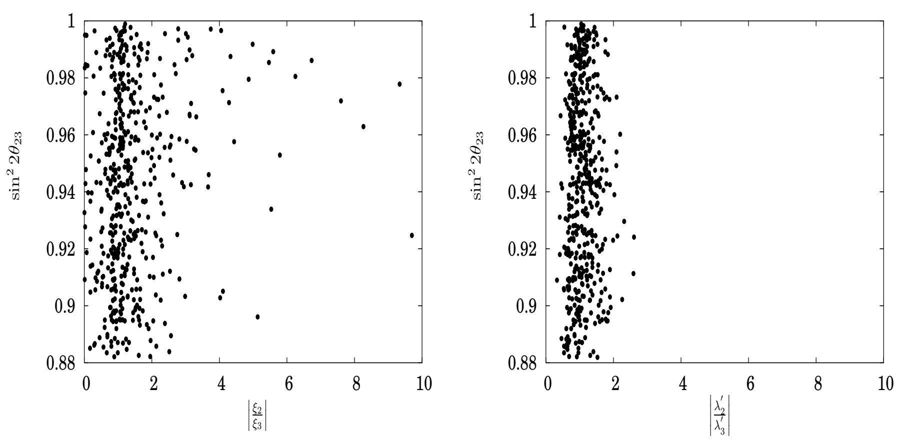

(a) $\sin^2 2\theta_{23}$ vs. $|\xi_2/\xi_3|$

(b) $\sin^2 2\theta_{23}$ vs. $\left|\lambda'_2/\lambda'_3\right|$

FIG. 6: The correlation between the atmospheric neutrino mixing angle and $|\xi_2/\xi_3|$ or $|\lambda'_2/\lambda'_3|$ for solution points with $\tan\beta = 3 - 15$.

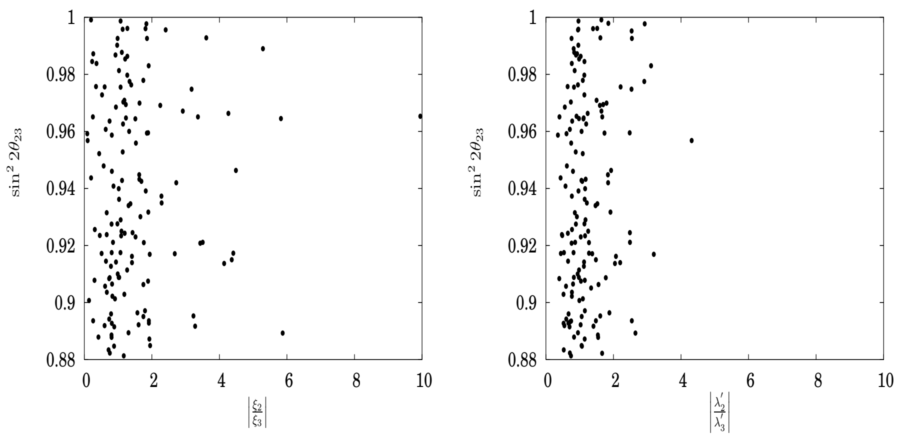

(a) $\sin^2 2\theta_{23}$ vs. $|\xi_3/\xi_3|$

(b) $\sin^2 2\theta_{23}$ vs. $\left|\lambda'_2/\lambda'_3\right|$

FIG. 7: Same figure as above but with $\tan\beta = 30 - 40$.

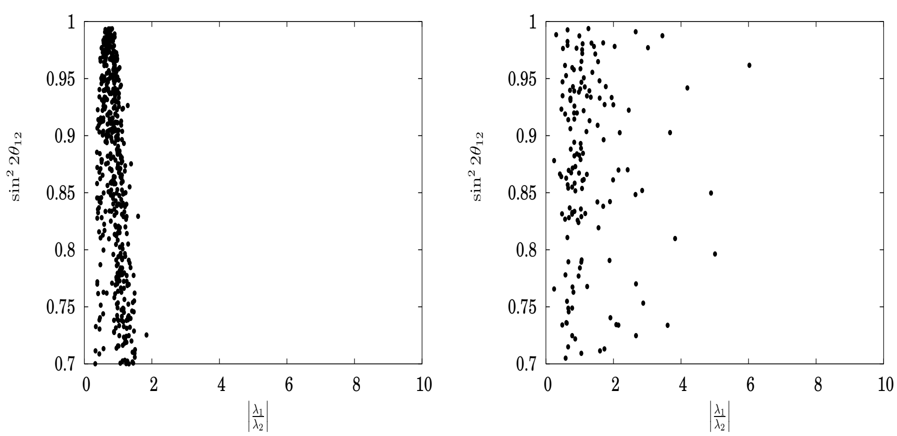

(a) $\sin^2 2\theta_{12}$ vs. $|\lambda_1/\lambda_2|$.

(b) $\sin^2 2\theta_{12}$ vs. $|\lambda_1/\lambda_2|$.

FIG. 8: The correlation between solar neutrino mixing angle and $|\lambda_1/\lambda_2|$ for solution points with (a) $\tan\beta = 3 - 15$ and (b) $\tan\beta = 30 - 40$.

	Stau LSP		
	$\tan\beta = 5.2$	$\mathrm{sgn}(\mu) = -1$	$\mu = -801.2$ GeV
	$A_0 = 39.5$GeV	$m_0 = 105.0$ GeV	$M_{1/2} = 671.0$ GeV
λ'_i	8.40×10^{-6}	-7.66×10^{-5}	-6.79×10^{-5}
λ_i	8.74×10^{-5}	-7.44×10^{-5}	0
ξ_i	-9.90×10^{-7}	-3.05×10^{-6}	-3.73×10^{-6}
η_i	1.01×10^{-6}	-1.31×10^{-5}	-1.19×10^{-5}
BR	e	μ	τ
$l_i\nu$	28.9 %	21.0 %	50.0 %
$\bar{t}\ b$		~ 0.07 %	
	$m_{\tilde{\tau}_1}$=278.6 GeV		$\Gamma = \ 2.92 \times 10^{-7}$ GeV
	$\sigma_{e^+e^- \to \tilde{\tau}_1\tilde{\tau}_1^*} \simeq 1.45\ \times 10^{-2}$ (Pb),	$\sqrt{s} = 1$ TeV	

$(\Delta m^2_{31},\ \Delta m^2_{21}) = (2.5 \times 10^{-3},\ 1.1 \times 10^{-4})$ eV^2
$(\sin^2 2\theta_{atm},\ \sin^2 2\theta_{sol},\ \sin^2 2\theta_{chooz}) = (0.98,\ 0.77,\ 0.03)$
The decay length $L \simeq 6.74 \times 10^{-8} cm$

TABLE I: A solution set with the stau LSP. The values of the trilinear couplings $\tilde{\lambda}'_i$ and $\tilde{\lambda}_i$ are taken as input parameters defined at the weak scale.

	Stau LSP		
	$\tan\beta = 38.0$	$\mathrm{sgn}(\mu) = -1$	$\mu = -460.1$ GeV
	$A_0 = 679.0$GeV	$m_0 = 233.4$ GeV	$M_{1/2} = 462.1$ GeV
λ'_i	1.53×10^{-6}	-1.48×10^{-5}	-5.84×10^{-6}
λ_i	3.65×10^{-6}	5.41×10^{-6}	0
ξ_i	-7.76×10^{-6}	-2.81×10^{-5}	-2.30×10^{-6}
η_i	8.17×10^{-6}	-3.38×10^{-5}	-1.73×10^{-5}
BR	e	μ	τ
$l_i\nu$	11.5 %	25.5 %	47.2 %
$\bar{t}\ b$		~ 16.0 %	
	$m_{\tilde{\tau}_1}$=188.7 GeV		$\Gamma = \ 7.99 \times 10^{-10}$ GeV
	$\sigma_{e^+e^- \to \tilde{\tau}_1\tilde{\tau}_1^*} \simeq 1.96\ \times 10^{-2}$ (Pb),	$\sqrt{s} = 1$ TeV	

$(\Delta m^2_{31},\ \Delta m^2_{21}) = (2.5 \times 10^{-3},\ 4.6 \times 10^{-5})$ eV^2
$(\sin^2 2\theta_{atm},\ \sin^2 2\theta_{sol},\ \sin^2 2\theta_{chooz}) = (0.99,\ 0.74,\ 0.005)$
The decay length $L \simeq 2.47 \times 10^{-5} cm$

TABLE II: Same as the previous table but with large $\tan\beta$.

	Neutralino LSP		
	$\tan\beta = 4.9$	$\mathrm{sgn}(\mu) = -1$	$\mu = -200.5$ GeV
	$A_0 = 38.9$GeV	$m_0 = 333.7$ GeV	$M_{1/2} = 160$ GeV
λ'_i	-9.33×10^{-9}	-7.81×10^{-5}	-7.56×10^{-5}
λ_i	-5.63×10^{-5}	-7.35×10^{-5}	0
ξ_i	-1.21×10^{-6}	2.75×10^{-7}	1.83×10^{-6}
η_i	-2.01×10^{-6}	-1.17×10^{-5}	-8.74×10^{-6}
BR	e	μ	τ
νjj		47.0 %	
$l_i^{\pm} jj$	3.88 $\times 10^{-2}$ %	2.00 $\times 10^{-3}$%	8.87 $\times 10^{-2}$%
$\nu l_i^{\pm} \tau^{\mp}$	9.8 %	16.6 %	26.4 %
	$m_{\tilde{\chi}_1^0}$=59.4 GeV		$\Gamma = 7.14 \times 10^{-15}$ GeV
	$\sigma_{e^+e^- \to \tilde{\chi}_1^0 \tilde{\chi}_1^0} \simeq 4.90 \times 10^{-2}$ (Pb),		$\sqrt{s} = 1$ TeV

$(\Delta m_{31}^2,\ \Delta m_{21}^2) = (2.5 \times 10^{-3},\ 9.6 \times 10^{-5})$ eV^2
$(\sin^2 2\theta_{atm},\ \sin^2 2\theta_{sol},\ \sin^2 2\theta_{chooz}) = (0.98,\ 0.99,\ 0.008)$
The decay length $L \simeq 2.76cm$

TABLE III: A solution set with the neutralino LSP which is lighter than the W boson.

	Neutralino LSP		
	$\tan\beta = 4.2$	$\mathrm{sgn}(\mu) = -1$	$\mu = -442.3$ GeV
	$A_0 = 98.5$GeV	$m_0 = 235.9$ GeV	$M_{1/2} = 380.9$ GeV
λ'_i	-1.18×10^{-8}	-1.44×10^{-4}	-1.47×10^{-4}
λ_i	-8.57×10^{-5}	-9.71×10^{-5}	0
ξ_i	3.24×10^{-7}	-8.37×10^{-7}	-1.17×10^{-6}
η_i	-6.72×10^{-7}	-1.73×10^{-5}	-1.68×10^{-5}
BR	e	μ	τ
νjj		30.1%	
$l_i^{\pm} jj$	3.14×10^{-2}%	2.10×10^{-1}%	4.08×10^{-1}%
$\nu l_i^{\pm} \tau^{\mp}$	15.1 %	19.4 %	34.4 %
$l_i^{\pm} W^{\mp}$	2.35×10^{-2}%	1.57×10^{-1}%	3.04×10^{-1}%
	$m_{\tilde{\chi}_1^0}$= 165.8 GeV		$\Gamma = 5.36 \times 10^{-12}$ GeV
	$\sigma_{e^+e^- \to \tilde{\chi}_1^0 \tilde{\chi}_1^0} \simeq 0.12$ (Pb),		$\sqrt{s} = 1$ TeV

$(\Delta m_{31}^2,\ \Delta m_{21}^2) = (2.5 \times 10^{-3},\ 6.5 \times 10^{-5})$ eV^2
$(\sin^2 2\theta_{atm},\ \sin^2 2\theta_{sol},\ \sin^2 2\theta_{chooz}) = (0.99,\ 0.96,\ 0.001)$
The decay length $L \simeq 3.67 \times 10^{-3}cm$

TABLE IV: A solution set with the neutralino LSP which is heavier than the W boson but lighter than the top quark

	Neutralino LSP		
	$\tan\beta = 7.6$	$\mathrm{sgn}(\mu) = -1$	$\mu = -832.3$ GeV
	$A_0 = 48.2$GeV	$m_0 = 255.4$ GeV	$M_{1/2} = 715.3$ GeV
λ'_i	-5.48×10^{-6}	-4.99×10^{-5}	-7.26×10^{-5}
λ_i	-5.00×10^{-5}	-6.22×10^{-5}	0
ξ_i	2.12×10^{-6}	7.66×10^{-6}	8.53×10^{-6}
η_i	-3.41×10^{-7}	-5.84×10^{-6}	-9.05×10^{-6}
BR	e	μ	τ
νjj		11.6%	
$l_i^{\pm} jj$	$1.82{\times}10^{-1}$ %	2.37 %	2.95 %
$l_i^{\pm}(tb)$	5.81×10^{-2}%	1.65%	3.13%
$\nu l_i^{\pm} \tau^{\mp}$	14.8 %	22.9 %	37.0 %
$l_i^{\pm} W^{\mp}$	1.35×10^{-1}%	1.77 %	2.19 %
	$m_{\tilde{\chi}_1^0}$=315.5 GeV		$\Gamma = 2.14 \times 10^{-11}$ GeV
	$\sigma_{e^+e^- \to \tilde{\chi}_1^0 \tilde{\chi}_1^0} \simeq 0.14$ (Pb),		$\sqrt{s} = 1$ TeV

$(\Delta m^2_{31},\ \Delta m^2_{21}) = (2.5 \times 10^{-3},\ 2.2 \times 10^{-5})\ \mathrm{eV}^2$
$(\sin^2 2\theta_{atm},\ \sin^2 2\theta_{sol},\ \sin^2 2\theta_{chooz}) = (0.91,\ 0.97,\ 0.05)$
The decay length $L \simeq 9.23 \times 10^{-4} cm$

TABLE V: A solution set with the neutralino LSP which is heavier than the top quark but lighter than two top quarks.

	Neutralino LSP		
	$\tan\beta = 9.7$	$\mathrm{sgn}(\mu) = -1$	$\mu = -1045.8$ GeV
	$A_0 = 526.5$GeV	$m_0 = 308.5$ GeV	$M_{1/2} = 947.6$ GeV
λ'_i	9.00×10^{-6}	6.54×10^{-5}	-7.61×10^{-5}
λ_i	6.40×10^{-5}	7.51×10^{-5}	0
ξ_i	-3.49×10^{-6}	6.97×10^{-6}	-3.82×10^{-6}
η_i	-3.56×10^{-6}	1.96×10^{-5}	-2.12×10^{-5}
BR	e	μ	τ
$\nu t\bar{t}$		97.8%	
$l_i^{\pm} jj$	$4.6{\times}10^{-3}$ %	$1.8{\times}10^{-2}$%	$5.5{\times}10^{-3}$%
$l_i^{\pm}(tb)$	1.6×10^{-3}%	3.3×10^{-2}%	4.3×10^{-2}%
$\nu l_i^{\pm} \tau^{\mp}$	4.3×10^{-1} %	5.9×10^{-1} %	1.02 %
$l_i^{\pm} W^{\mp}$	3.39×10^{-3}%	1.35×10^{-2} %	4.05×10^{-3} %
	$m_{\tilde{\chi}_1^0}$=417.0 GeV		$\Gamma = 2.04 \times 10^{-9}$ GeV
	$\sigma_{e^+e^- \to \tilde{\chi}_1^0 \tilde{\chi}_1^0} \simeq 1.04 \times 10^{-1}$ (Pb),		$\sqrt{s} = 1$ TeV

$(\Delta m^2_{31},\ \Delta m^2_{21}) = (3.6 \times 10^{-3},\ 3.2 \times 10^{-5})\ \mathrm{eV}^2$
$(\sin^2 2\theta_{atm},\ \sin^2 2\theta_{sol},\ \sin^2 2\theta_{chooz}) = (0.96,\ 0.98,\ 0.03)$
The decay length $L \simeq 9.66 \times 10^{-6} cm$

TABLE VI: A solution set with the neutralino LSP which is heavier than two top quarks.